2009

DESIGN AND ANALYSIS OF NANO-GAP ENHANCED SURFACE PLASMON RESONANCE SENSORS

Phillip Donald Keathley
University of Kentucky, dkeathley@gmail.com

ABSTRACT OF THESIS

DESIGN AND ANALYSIS OF NANO-GAP ENHANCED SURFACE PLASMON RESONANCE SENSORS

Surface plasmon resonance (SPR) sensors are advantageous to other techniques of sensing chemical binding, offering quantitative, real-time, label-free results. Previous work has demonstrated the effectiveness of using dual-mode SPR sensors to differentiate between surface and background effects, making the sensors more robust to dynamic environments. This work demonstrates a technique that improves upon a previously optimized planar film dual-mode SPR sensor's LOD by introducing a periodic array of subwavelength nano-gaps throughout the plasmon supporting material. First, general figures of merit for a sensor having an arbitrary number of modes are studied. Next, the mode effective index dispersion and magnetic field profiles of the two strongly bound modes found using a gap width of 20nm are analyzed. Qualitative analysis of the results demonstrates how such a design can enable better LODs in terms of each figure of merit. By optimizing a nano-gap enhanced sensor containing 20nm gaps, it is quantitatively demonstrated that the resulting modes improve upon almost every figure of merit, especially with respect to the orthogonality and magnitude of the sensitivity vectors, resulting in LODs approximately a factor of five less than the optimal planar design.

KEYWORDS: Surface Plasmon Resonance, Biosensor, Nano-Gaps, Optimization, Limit of Detection

Donnie Keathley, 8-4-2009

DESIGN AND ANALYSIS OF NANO-GAP ENHANCED SURFACE PLASMON RESONANCE SENSORS

By

Phillip Donald Keathley

Dr. J. Todd Hastings
Director of Thesis

Dr. Stephen Gedney
Director of Graduate Studies

8-4-2009

RULES FOR THE USE OF THESES

Unpublished theses submitted for the Master's degree and deposited in the University of Kentucky Library are as a rule open for inspection, but are to be used only with due regard to the rights of the authors. Bibliographical references may be noted, but quotations or summaries of parts may be published only with the permission of the author, and with the usual scholarly acknowledgments.

Extensive copying or publication of the thesis in whole or in part also requires the consent of the Dean of the Graduate School of the University of Kentucky.

A library that borrows this thesis for use by its patrons is expected to secure the signature of each user.

Name Date

_____

_____

_____

_____

_____

_____

_____

_____

_____

_____

_____

_____

_____

_____

THESIS

Phillip Donald Keathley

The Graduate School

University of Kentucky

2009

DESIGN AND ANALYSIS OF NANO-GAP ENHANCED SURFACE PLASMON RESONANCE SENSORS

THESIS

A thesis submitted in partial fulfillment of the
requirements for the degree of Master of Science in
Electrical Engineering in the College of Engineering
at the University of Kentucky

By Phillip Donald Keathley

Lexington, KY

Director: Dr. J. Todd Hastings, Professor of Electrical Engineering

Lexington, KY

2009

This work is dedicated to my parents.

ACKNOWLEDGEMENTS

It would be entirely unfair if I did not write a few words to thank all of the people that helped so much in making this work possible. First, I would like to thank my advisor, Dr. Todd Hastings, for his assistance, experienced insight, and, most importantly, for helping me to be confident of my own ideas throughout this project. Dr. Chuck May and Brian Wadjyk with the Center for Nanoscale Science and Engineering at the University of Kentucky were a major help during the fabrication process, and had much patience throughout hectic scheduling. Without guidance and assistance from Vinayak Bhat, I probably would not have been able to deposit the necessary thin films of HSQ in time for this project. While we did not work together on this project, collaboration with Jing Guo on previous SPR sensor projects helped me to learn much of what I know about designing and fabricating working sensors. I would also like to thank everyone else in the lab, as I'm quite positive that everyone has helped me in some form or fashion with this project, or one of the many others leading up to it. Lastly, I could not have begun any of this if it were not for the support and encouragement from family friends and loved ones outside of the lab.

TABLE OF CONTENTS

LIST OF TABLES

LIST OF FIGURES

Chapter 1: Introduction

Surface plasmon resonance (SPR) sensors provide label free and real time analysis of optical property changes near a metal-dielectric interface that supports surface plasmons. Surface plasmons are propogating or localized electromagnetic field oscillations that occur at the interface between two materials given that one of the materials has a real negative dielectric constant.[1, 2] In most sensor applications the plasmon supporting material is gold or silver as they readily support plasmon modes. The adjacent material is typically a liquid with a refractive index near that of water hereafter referred to as the analyte solution. For a given plasmon wave vector, k_{sp}, plasmon modes are only supported for a discrete number of eigenfrequencies each having a dispersion curve defined by $\omega(k_{sp})$.[2] As with any propogating mode, this dispersion relationship can be perturbed by changes in the material properties near locations where the mode's electromagnetic field values are significant, at the metal-analyte interface for SPR sensors. The means of tracking changes in the dispersion of plasmon modes due to perturbation will be discussed in detail, but it is important to quickly ask why being able to track these changes is important, and why and/or when it would be preferred over other means of detection.

In practice, SPR sensing is most commonly used to detect biological analytes that bind to the sensor surface, and to analyze the physics behind biomolecular interactions occurring at or near the interface of propogation. SPR sensors are advantageous to other methods, such as fluorescent tagging, when a quantitative label-free approach to tracking binding occurrences or optical property shifts over time is needed. [3] While their

usefulness in the areas of medical and pharmaceutical research are the major impetus behind the creation of commercial SPR sensing equipment, such as the Biacore line of SPR sensor units (GE Healthcare), SPR sensors have been utilized in the measurement of angular position, humidity and temperature sensing due to their high sensitivity to slight changes in refractive index in the past.[4] It is hoped that further development of robust multi-moded SPR sensors similar to those presented in this work will push the usefulness of SPR sensors beyond their current applications in the research laboratory and into more common areas where the optical properties of the environment (i.e. temperature and concentration shifts) can fluxuate greatly over time. Many fields, such as water quality testing, could benefit from the real-time quantitative detection of small chemical concentrations, but require the sensors to function properly in such fluctuating analyte solutions.

Most useful surface plasmon modes have a wave vector that lies to the right of the light line, meaning that it is impossible to directly couple to a mode by shining light on a structure supporting surface plasmons. In order to circumvent this problem, there are two prevalent techniques for increasing the wave vector of incoming light to achieve plasmon coupling: diffraction and attenuated total reflection (ATR). Figure 1.1 shows a schematic of each. Each configuration serves the purpose of increasing k_x of the incoming light so that at a certain angle and frequency it will cross the dispersion curve of k_{sp}. In this work we will deal solely with the ATR setup, however it should be noted that the designs proposed in this thesis could also utilize diffracted orders as a means of coupling.

Figure 1.2a presents a plot of the disperision curve of a plasmon mode propogating along the interface of an infinitely thick film of gold and a water analyte

solution along with the dispersion curve of incident light in the x-direction at an angle of 70° inside a BK7 glass prism. The analytic expressions for the dispersion curves plotted are taken to be

$$n_{sp} = \mathrm{Re}\left[\left(\frac{\varepsilon_d \varepsilon_m}{\varepsilon_d + \varepsilon_m}\right)^{1/2}\right] \tag{1.1}$$

$$n_{inc,x} = n_{inc}\sin(\theta_{inc}) \tag{1.2}$$

with n_{sp} here being the real part of the plasmon effective index of refraction (only real part is analyzed for phase matching), ε_d and ε_m the dielectric constants of the dielectric material (analyte solution) and metal film respectively, $n_{inc,x}$ the effective index in the x-direction of the light traveling in the incident material (BK7 glass) having an index of n_{inc} and angle of incidence θ_{inc}.

Figure 1.2b plots the reflectivity of light traveling in a BK7 glass prism incident after striking a 60nm thick gold film covered by a water analyte solution. Since the dip in reflectivity seen in figure 1.2b so closely corresponds to the intersection between the dispersion curves presented in figure 1.2a, the infinite film approximation is taken to hold, and the dip is attributed to plasmon mode coupling due to phase matching. It should be noted here that surface plasmon resonance is a purely transverse magnetic (TM) phenomenon, meaning that no modes are found to couple in a transverse electric (TE) configuration. This is due to the fact that surface plasmons depend on fluctuations of charge density, which requires an electric field component normal to the surface of the plasmon supporting material. This property of surface plasmons allows for the TE reflectivity to be used in all reflectivity plots as a reference spectrum.

By fixing the angle of the incident light, one is able to track the minimum in figure 1.2(b) over time. If the minimum shifts, then something has perturbed the plasmon mode. Suppose the surface of the sensor is coated by a layer of receptor chemicals as seen in figure 1.3(a). If a solution with a chemical that binds strongly to the receptor was used as the analyte, one could then track the minimum shift over time and know whether or not binding occurred, the rate and the extent of binding all by tracking the minimum shift over time. Figure 1.3(b) shows the shift due to the binding of a 2nm surface layer of uniform refractive index. However, the difficulty in this situation is ensuring no drift in background (analyte solution) refractive index (due to temperature or concentration shifts) and having a well-calibrated sensitivity value to determine the exact amount of binding on the surface. Typically, and in the entirety of this work, all perturbations are assumed to shift the coupling wavelength/angle in a linear fashion.

While having temperature and concentration controlled analyte solutions is possible in a laboratory situation, in order to create more robust sensors that have potential outside of laboratory use, it becomes necessary to conceive of sensor designs that can account for change due to both the perturbation of interest such as surface binding, and perturbations due to other causes. This requires the use of more than a single mode, which can be achieved directly by creating sensors that support multiple plasmon resonances.

We have demonstrated that dual mode SPR sensors can be used to successfully determine shifts due to background index changes and surface binding occurrences simultaneously.[5, 6] These sensors use a thin dielectric layer sandwiched between the glass substrate and the gold film to produce a near symmetric index profile normal to the

sensor surface. With thin gold films, two modes are supported at different wavelengths[1], one having a magnetic field profile that is symmetric about the metal film, and one having a magnetic field profile that is anti-symmetric about the metal film. Due to differing field profiles in the analyte solution, each mode has a differing sensitivity to surface and background change thus making it possible to differentiate between the two. Figure 1.4 gives a schematic of the sensor design along with the reflectivity spectrum and field profiles in the materials. Magnetic field profiles are plotted for simplicity as there is only a single magnetic field component in y for plasmons and the profiles of the electric and magnetic fields correspond with one another, as they are exponential in nature.

There is an inconsistency in the SPR community regarding the performance comparison of sensors. Many tend to optimize by maximizing sensitivity to the perturbation of interest. However it has been shown that such an optimization can in fact be misleading as it ignores one's limitations in determining and tracking reflectivity minima.[7, 8] A more comprehensive figure of merit is the sensor's limit of detection (LOD) which quantifies the smallest amount of a given perturbation that is detectable by the sensor as being three standard deviations of the measured value (i.e. the smallest analyte refractive index change, or the thinnest bound film detectable). Others have shown that a theoretical minimum variance for spectral peak/minimum shift tracking can be calculated by utilizing the Cramer Rao lower bound for variance.[8, 9] Their results depend on Poisson counting noise, which is typically the case for CCD based spectrometers at high intensity, but could also be developed for various noise

distributions. For the case of dual mode sensors, we have used this calculation to optimize single and dual mode sensor performance in terms of LOD.[8, 10]

The work presented in this thesis attempts to gain a better understanding of what sensor characteristics lead to better LODs, and provides a means of increasing sensor performance in terms of LOD by introducing periodic subwavelength nano-gaps in the metal film of previous dual mode designs as seen in figure 1.5. This design was chosen for three main reasons. First, the presence of the gaps significantly alters the dispersion relationship of supported plasmon modes. This alters both the full width at half minimum (FWHM) of the resonance dips in the reflectivity spectrum and the sensitivity of the mode to perturbations. Others have noticed similar effects when using traditional SPR sensors with nanowires superimposed on the surface.[11] This structure also supports propogating modes that are more slit confined in nature which are present no matter how small of a gap is introduced in the plasmon supporting film.[12] As opposed to the surface modes, which peak in field strength along the plasmon supporting film and have evanescent waves that extend into the surrounding dielectrics, the slit confined modes peak in field strength in the center of the slit and can be extremely confined to the slit with very weak evanescent fields that extend into either dielectric. In keeping with the terminology used in [12] the slit confined modes will be hereafter referred to as "effective dielectric slab modes." These new modes make it possible to engineer sensors that have more orthogonal sensitivities than previous planar sensor designs (see later analysis). The third reason is due to electric field enhancement of the plasmon modes to a greater extent within the gaps as is observed with finite element modeling of the

structures, which could also be utilized in creating more orthogonal sensitivity vectors with larger magnitudes.

The most prevalent materials utilized by the dual mode sensors, Teflon and gold, will be used here as they present near ideal optical properties for coupling to plasmon modes with analyte solutions near the index of water. As more modes are possible using the nano-gap based sensors, there was reason to approach the LOD calculation from a more general standpoint of multiple modes and multiple perturbation values to solve for simultaneously. The slits also give many more free parameters to adjust for optimal performance opening up new engineering possibilities, but making for a much more involved optimization process. However, even by limiting the free parameters for the optimization search, it was found that surface layer LOD and background LOD values can be decreased by approximately a factor of five when compared to the optimal dual mode values presented in [10]. It is hoped that future work can use the findings presented here to further engineer SPR sensors having mode field profiles that better approach an optimal design from the standpoint of LOD.

(a)

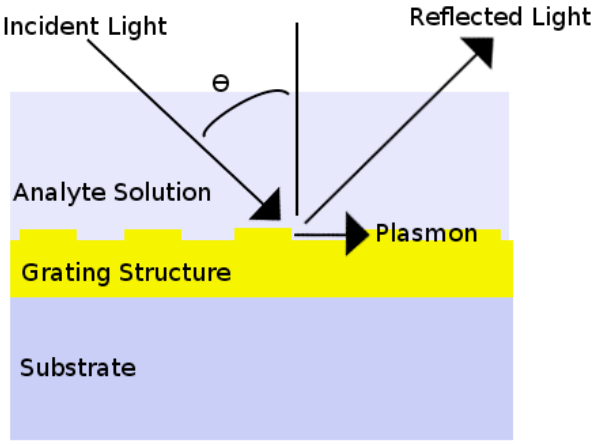

(b)

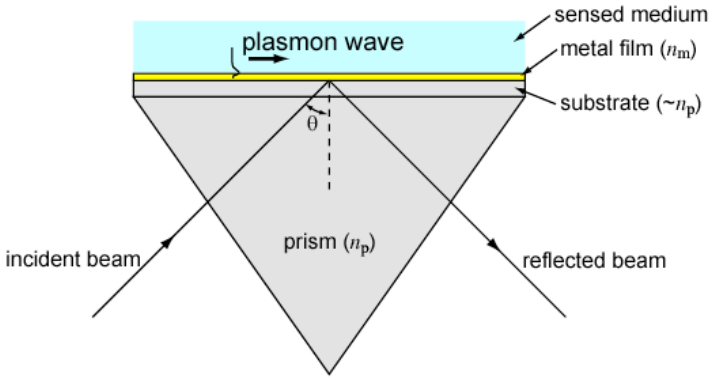

Figure 1.1 – Diffraction and ATR Coupling Schematics. (a) A diffraction grating coupled SPR sensor and (b) the ATR coupled SPR sensor. While the prism mount is necessary to increase the momentum of the incident light in the x direction for SPR coupling in the ATR setup, the periodic structure of the grating creates evanescent waves on the surface of higher x-momentum that couple to the plasmon mode of the supporting material.

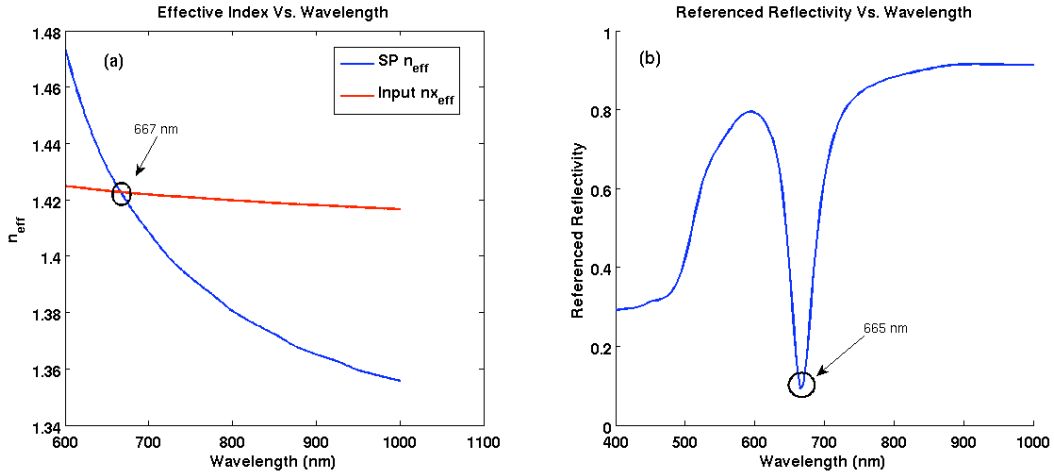

Figure 1.2 - Single Mode Dispersion Matching, Single Mode Resonance Dip. (a) Plot of effective index (n_{eff}) vs. wavelength for a plasmon mode in a single mode sensor, using the approximation of an infinitely thick gold film covered with water. Also shown is the effective index, in the x direction, of incident light in the prism at an angle of 70°. (b) A plot of the reflectivity of TM incident light referenced by the TE reflectivity as a function of wavelength for the case of 60 nm of gold deposited on glass with water as the analyte in the ATR arrangement. Note that the reflectivity minimum shown corresponds to the intersection point of the two dispersion curves in (a).

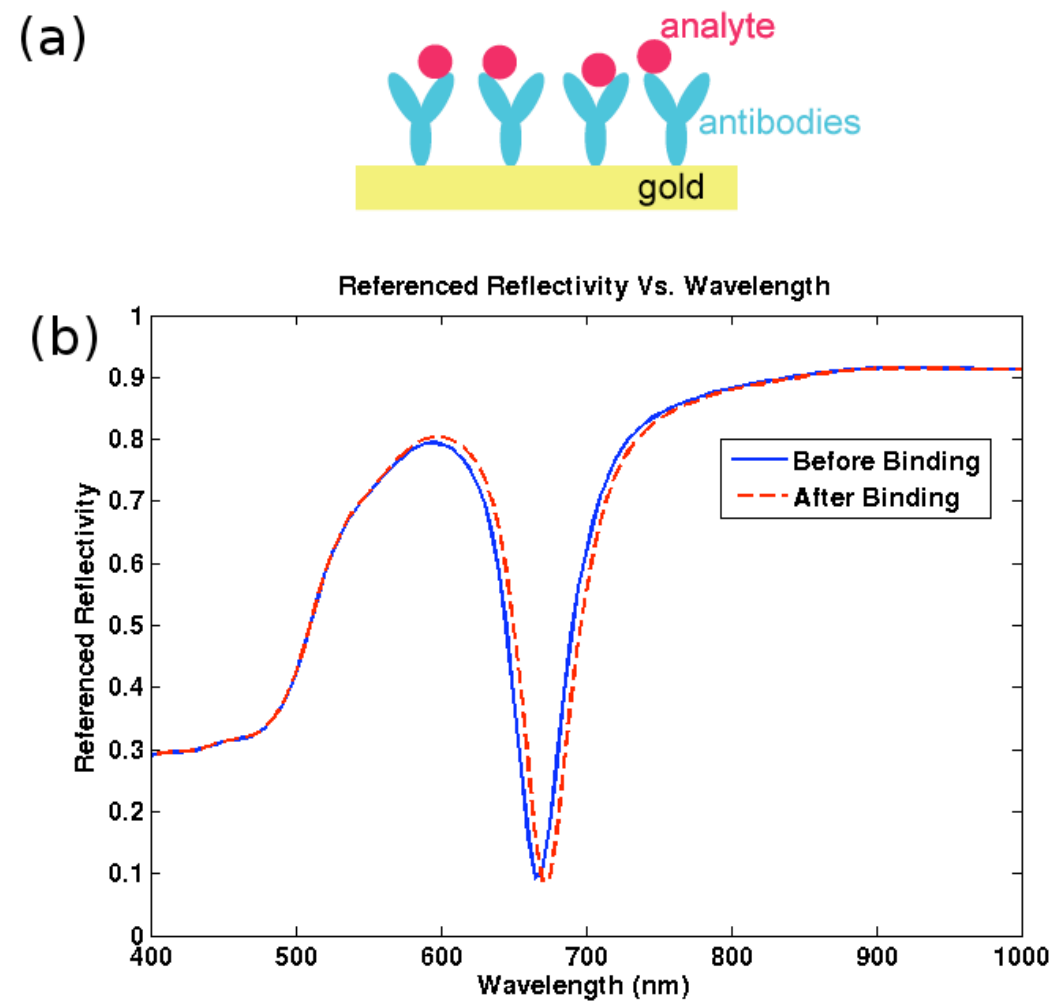

Figure 1.3 – Surface Binding and Single Mode Resonance Shift. (a) Schematic of the sensor surface functionalized for specific binding by being coated with chemical receptors. (b) Plot of referenced reflectivity vs. wavelength for the same sensor used in figure 1.2 before and after binding of a 2nm thick surface layer having a uniform refractive index of 1.45.

(a)

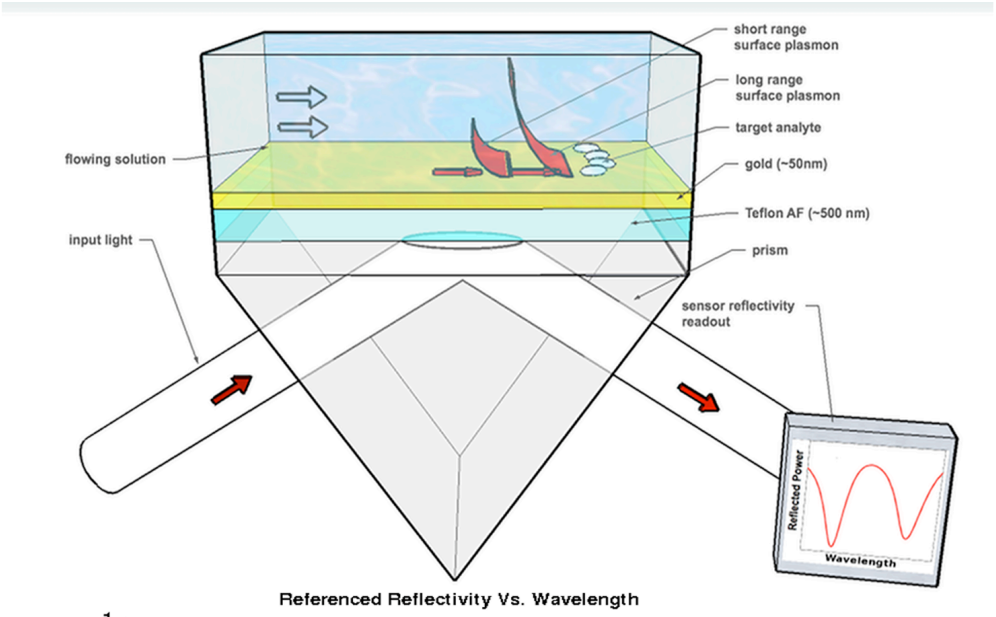
short range
surface plasmon
long range
surface plasmon
target analyte
flowing solution
gold (~50nm)
Teflon AF (~500 nm)
input light
prism
sensor reflectivity
readout
Reflected Power
Wavelength

(b)

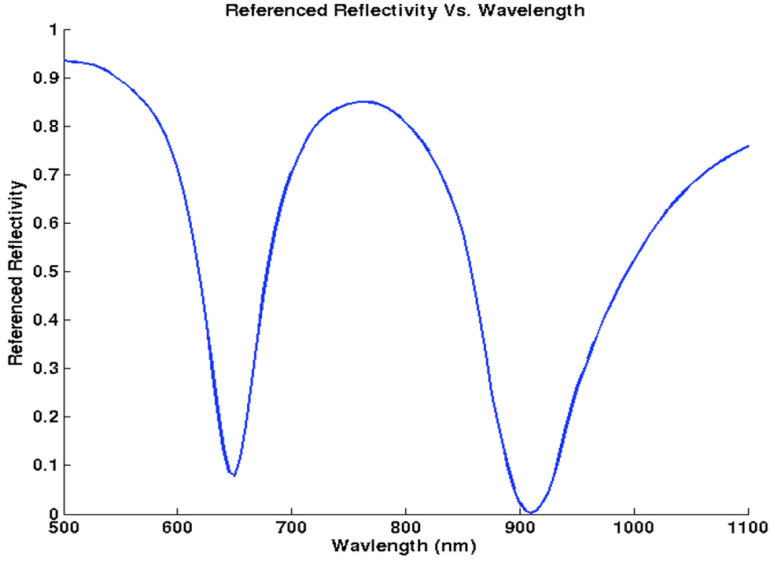
Referenced Reflectivity Vs. Wavelength
Referenced Reflectivity
Wavlength (nm)

(c)

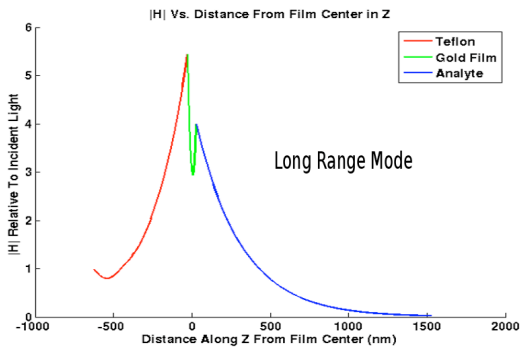
|H| Vs. Distance From Film Center in Z
Teflon
Gold Film
Analyte
Long Range Mode
|H| Relative To Incident Light
Distance Along Z From Film Center (nm)

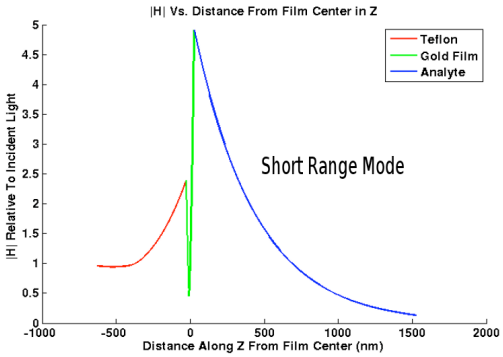
|H| Vs. Distance From Film Center in Z
Teflon
Gold Film
Analyte
Short Range Mode
|H| Relative To Incident Light
Distance Along Z From Film Center (nm)

Figure 1.4 – ATR Dual-Mode Schematic, Dual-Mode Reflectivity, and Mode Magnetic Field Profiles. (a) Schematic of the planar film dual-mode SPR sensor design using gold and Teflon. (b) Referenced reflectivity vs. wavelength for a dual mode planar sensor with a gold thickness of 55 nm, a Teflon thickness of 400 nm and an incident angle of 65.5°. The long range mode corresponds to the dip at 650 nm, and the short range to the dip at 910 nm. (c) & (d) Field profile of $|H_y|$ as a function of z from the center of the gold film for the long range and short range mode respectively. There is a zero crossing in the film for the short range mode making it anti-symmetric about x.

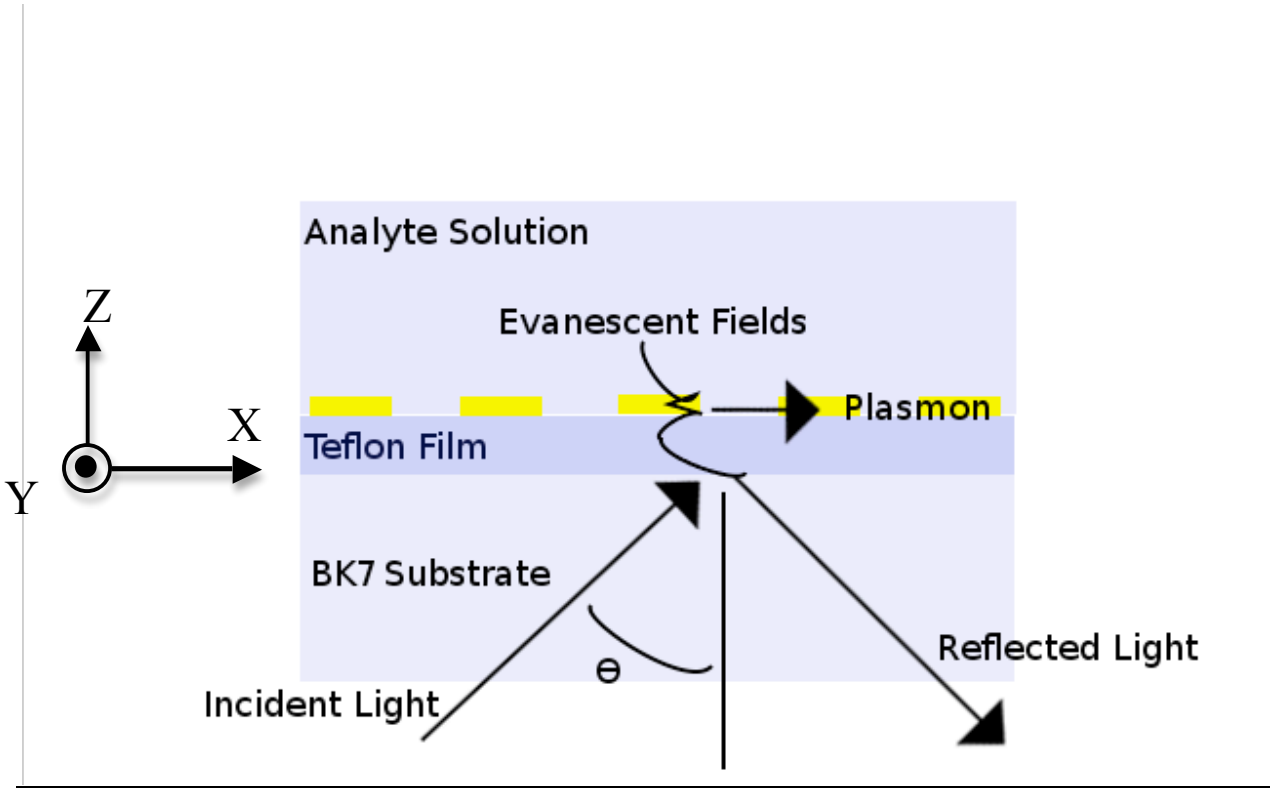

Figure 1.5 – Nano-Gap Enhanced Design Schematic. Due to the addition of periodic nano-gaps within the metal film, additional electromagnetic modes are present which can be utilized to improve sensitivity and reduce the sensor's LOD. The coordinate conventions used for the rest of the paper are also defined here.

Chapter 2: Analysis and Optimization Procedures

Solving for Perturbation Values - The General Case

As earlier stated, the nano-gap enhanced sensor can support many modes not present in the case of a planar thin-film SPR sensor. This gives reason for developing equations that are more general in approach, accounting for n perturbations and m modes. From this point forward, the term perturbation will be used to specify any occurance that causes a shift in a plasmon mode dispersion profile that can be solved for (i.e. background index shift or surface layer binding). To avoid confusion, the use of short- and long- range plasmon terminology will also be avoided, as with the nano-gap enhanced case it would be too difficult to give distinct names to the various modes possible. In fact, it has been seen that for very thin films with nano-gaps, there exists many modes that are not purely surface or dielectric slab modes but a mixture of both, being distinguished by their profiles along the film (peak values in either the slit or the metal film) and normal to the film (either symmetric or anti-symmetric).[12]

Assuming that all perturbations to the plasmon modes shift each resonance point in a linear fashion, the following equation can be used to describe all of the resonance shifts present when there are n perturbations and m modes.

$$\mathbf{SP} = \Delta\lambda \tag{2.1}$$

$\mathbf{S}$ is taken to be an $m \times n$ sensitivity matrix made up of n sensitivity vectors, $\mathbf{P}$ a $n \times 1$ perturbation vector, and $\Delta\lambda$ a $m \times 1$ vector of resonance wavelength shifts. The

perturbation amounts can easily be approximated using the least squares solution to the above matrix whenever $m \geq n$.

$$\mathbf{P} = (\mathbf{S}'\mathbf{S})\mathbf{S}'\Delta\lambda \tag{2.2}$$

With an ideal sensor, only $m = n$ modes are necessary, as adding further modes would not provide additional data. In this work it is assumed that the sensors can be treated as ideal, which is typically sufficient for careful testing. However, it should be noted that in situations where there is greater room for error in determining resonance shifts, using more modes would provide a better approximation of the perturbation values.

For the nano-gap enhanced SPR sensors presented in this work, only two modes are typically prevalent. However, it should be noted that in some cases more modes may present themselves and are utilized when found. For the analysis presented here, it is assumed that two main perturbations are the only cause of resonance wavelength shifts, one due to a background index change (in the analyte solution), and one due to surface layer binding. Taking $\mathbf{S}_n = \begin{bmatrix} S_{n1} & S_{n2} \end{bmatrix}'$ as the background index sensitivity vector and $\mathbf{S}_t = \begin{bmatrix} S_{t1} & S_{t2} \end{bmatrix}'$ as the surface layer sensitivity vector and assuming two modes are present, equation (2.2) can be rewritten as follows.

$$\begin{bmatrix} \Delta n \\ \Delta t \end{bmatrix} = \frac{\begin{bmatrix} S_{n1}|\mathbf{S}_t|^2 - S_{t1}(\mathbf{S}_n \cdot \mathbf{S}_t) & S_{n2}|\mathbf{S}_t|^2 - S_{t2}(\mathbf{S}_n \cdot \mathbf{S}_t) \\ S_{t1}|\mathbf{S}_t|^2 - S_{n1}(\mathbf{S}_n \cdot \mathbf{S}_t) & S_{t2}|\mathbf{S}_t|^2 - S_{n2}(\mathbf{S}_n \cdot \mathbf{S}_t) \end{bmatrix}}{|\mathbf{S}_n|^2|\mathbf{S}_t|^2 - (\mathbf{S}_n \cdot \mathbf{S}_t)^2} \begin{bmatrix} \Delta\lambda_1 \\ \Delta\lambda_2 \end{bmatrix} \tag{2.3}$$

While a more simplified form of this equation has been presented by Hastings et al., it is is left in this form here as it highlights that the right hand side of the equation is inversely proportional to $|\mathbf{S}_n|^2|\mathbf{S}_t|^2 - (\mathbf{S}_n \cdot \mathbf{S}_t)^2$, which is maximized when $\mathbf{S}_n$ and $\mathbf{S}_t$ are orthogonal. This condition for maximum is true no matter how many modes are analyzed (it is inversely proportional to the Gram determinant, which is by definition the square of the volume of the n-dimensional parallelotope formed by the vectors and is thus maximized when they are orthogonal[13]). The importance of this result will be highlighted in the LOD derivation.

Determining LOD – The General Case

The LOD for measuring any perturbation value with an SPR sensor is taken to be three times the standard deviation of the perturbation value being measured.[8, 10] This reflects the smallest perturbation value that can be realistically detected by a sensor, and is calculated by utilizing the equations derived earlier for determining unknown perturbation values.

For the general case of m modes and n perturbations, the LOD can be related to the variance of $\mathbf{P}$ as follows with $\mathbf{LOD}$ taken to be an $n \times 1$ vector.

$$\mathbf{LOD} = 3\sqrt{\text{var}(\mathbf{P})} \tag{2.4}$$

To find $\text{var}(\mathbf{P})$ one can assume that all of the sensitivity matrix values are non-random (i.e. without noise), which correlates well to experimental results as these values can be determined by averaging the signal for a long period of time in a highly controlled environment. By using the following notation,

$$\mathbf{A}.^{\wedge 2} \equiv \begin{bmatrix} A_{11}{}^{2} & \cdots & A_{1n}{}^{2} \\ \vdots & \ddots & \vdots \\ A_{m1} & \cdots & A_{mn}{}^{2} \end{bmatrix}$$

one can represent var($\mathbf{P}$) by using equation (2.2)

$$\text{var}(\mathbf{P}) = \left[(\mathbf{S}'\mathbf{S})^{-1}\mathbf{S}'\right].^{\wedge 2} \text{var}(\Delta\lambda) \tag{2.5}$$

While data is available to determine var($\Delta\lambda$) in an experimental scenario, it is possible to also gain insight from equation (2.5) by using it to obtain a lower bound for the LOD for each unknown perturbation. This technique has been demonstrated by Hastings in the design of optimal single and dual mode SPR sensors [8, 10], and is an extension of work done by Karl and Pien in determining spectral peak shifts [9]. The lower bound of the LOD directly coincides with the lower bound of var($\Delta\lambda$), which is taken to be

$$\text{var}(\Delta\lambda_i) \geq \text{var}_{\min}(\Delta\lambda_i) = \left[\sum_{j=1}^{N}\left(\left.\frac{dR(\lambda)}{d\lambda}\right|_{\lambda=\lambda_j-\Delta\lambda_i}\right)^2 \frac{n_d(\lambda_j)}{R(\lambda_j-\Delta\lambda_i)}\right]^{-1} \tag{2.6}$$

Where $R(\lambda)$ is the reflectivity of the sensor as a function of λ, N is the number of samples taken around the i^{th} mode, and $n_d(\lambda_j)$ is the number of photons that would be detected in the λ_j sample of the spectrometer with $R(\lambda)=1$. This calculation assumes Poisson counting noise, which is generally applicable to silicon CCD detectors

commonly used with visible to near IR wavelength spectrometers in the presence of high light levels.

By using the assumption that the measurements of each resonance shift are uncorrelated, one can then represent the general minimum LOD vector by writing it in the following form.

$$\mathbf{LOD}_{\min} = 3\sqrt{\left[\left(\mathbf{S}'\mathbf{S}\right)^{-1}\mathbf{S}'\right].^{\wedge 2}\left[\mathrm{var}_{\min}(\Delta\lambda_1) \quad \cdots \quad \mathrm{var}_{\min}(\Delta\lambda_m)\right]'} \tag{2.7}$$

It is evident that equation (2.7) should be minimized for all perturbation values for an optimal sensor design. However, in realistic situations the minima for each element of the $\mathbf{LOD}_{\min}$ do not perfectly overlap. In this case, the perturbation of greatest interest, in our case surface binding, is optimized for while ensuring that other LOD values are within an acceptable tolerance.

Hastings showed that $\mathrm{var}_{\min}(\Delta\lambda_i)$ is minimized for low minimum reflectivities and low full width at half minimum (FWHM) of the resonance dips with the approximation that they have a Lorentzian line shape. [8] In general this conclusion should apply to any shape as deep, narrow dips will maximized the square of the derivative of the reflectivity in (2.6). However, our calculation shows that with multiple modes, the relationship with sensitivity becomes quite difficult to qualitatively analyze. However, going back to equation (2.3) there is an evident inverse relationship to the orthogonality and magnitude of the sensitivity vectors. A figure of merit that can be used for the orthogonality is the angle between the sensitivity vectorsMore interestingly, it

shows that even if a sensor has an incredibly high sensitivities to each perturbation, the effect is greatly diminished if the vectors all point very close to the same direction. In the two mode case, the figure of merit used to analyze the orthogonality is the angle between the sensitivity vectors given below.

$$\theta_{sens} = \cos^{-1}\left(\frac{\mathbf{S}_t \cdot \mathbf{S}_n}{|\mathbf{S}_t||\mathbf{S}_n|}\right) \tag{2.8}$$

The following table compiles all of the major figures of merit for a minimum LOD and their desired value (if there is not an exact value desired, it is specified whether the figure of merit should be low or high to achieve smaller LODs).

Table 2.1: LOD Figures of Merit

LOD Figure of Merit	**Desired Value for Minimum LOD**
FWHM of Resonance Dips	Low
Minimum Reflectivity of Resonance Dips	Low
Sensitivity Vector Magnitudes	High
Angle Between $\mathbf{S}_i$, $\mathbf{S}_j$ for $i \neq j$	90°

Chapter 3: Electromagnetic Simulation and LOD Analysis

Determination and Analysis of Mode Dispersion Profiles

While it is not necessary to know the dispersion curve of a plasmon mode to design a sensor, it can be very useful in understanding sensitivity and, by tracking the mode profile through the dispersion, how differing coupling locations can lead to differing sensor characteristics. For instance, a sensor has a greatly enhanced sensitivity in regions that the dispersion curve has similar slope to that of the incident dispersion curve as smaller perturbations in n_{eff} can lead to much larger shifts in the coupling wavelength, λ_{sp}.

Due to the variable periodic structure in x of the nano-gap enhanced sensor proposed, it is much more difficult to create an analytical solution describing each supported mode's dispersion profile. However, it has been shown that for an infinite periodic stratified medium, each solution to Maxwells equations is a superposition of a propogating and standing wave, in both the gap and the film region.[14] This has been observed when examining the mode propogation using the finite element method approach with Comsol and could be useful in terms of developing SPR sensors that are more "sensitive" in the region of the gap or the region of the film.

Without an analytical solution at hand, an iterative approach was employed using Comsol to determine each mode's dispersion profile. The structure used was identical to one isolated period of figure 1.5 with floquet (or bloch) periodic boundary conditions at the left and right hand boundaries and perfectly matched layers (PMLs) at the top and bottom boundaries. The floquet boundary conditions can be described mathematically as

$$H_y(x+\Lambda) = \exp(jk_{sp}\Lambda)H_y(x) \tag{3.1}$$

where H_y is the magnetic field in the y direction, $k_{sp} = \frac{2\pi n_{eff}}{\lambda_0}$ is the plasmon wave-vector and Λ is the length of one period of the structure. The plasmon wave-vector can be imaginary for leaky modes (which is inherent with plasmons due to the metal film). An eigenfrequency analysis was employed in the search process in order to locate eigenmodes of the structure corresponding to plasmon modes. However, this requires that the linearization setpoint in comsol be defined as the PMLs make the structure non-linear. The linearization setpoint should correspond to the complex component of the exponential equation corresponding to angular frequency that is close to the expected eigenfrequency solution, which is in our case simply $-j\frac{2\pi c}{\lambda_0}$. With a twice-refined default mesh, dispersion data very consistent with the exact solutions for plasmon modes in planar films was achieved as will be shown.

Comsol was used in conjunction with MATLAB to make the iteration process simpler to execute and material properties easier to define as a function of wavelength. Material properties for gold were taken from the measurements of Johnson and Christy[15] which provided a close match to experimental results in previous SPR sensing experiments.[10] The BK7 optical constants were found using the Sellmeier coefficients supplied by Schott North America Inc.[16], and the optical constants for Teflon-AF were calculated using the Cauchy dispersion formula fit to measurements of

Lowry et al.[17] For wavelengths not defined by the optical constants, a cubic polynomial fit was used for interpolation.

The algorithm used in calculating the dispersion profile is described as follows.

1) Using an initial guess for n_{eff}, the eigenfrequencies for the structure are determined using the material properties of each material at a starting wavelength of λ_0.
2) The returned eigenfrequencies are checked to determine if they fall within a set tolerance around $\frac{c}{\lambda_0}$, if not then then n_{eff} is shifted up/down and the process starts again. If yes, then the process moves to step 3.
3) This n_{eff} is stored. The next guess for n_{eff} is calculated by subtracting $n_{eff}(\lambda_0 - \Delta\lambda_0)$ from the $n_{eff}(\lambda_0)$ just found. Next, λ_0 is incremented by $\Delta\lambda_0$ and the process starts back at step 1.

To prevent the occurrence of and/or tracking of "false" modes, the PML layers were set to be absorbing only in the z direction (as diagrammed here, the y direction in Comsol), and only modes that exhibit field enhancment were accepted.

There were two major difficulties in this procedure. The first was to find good initial guesses for the effective indices. One successful method was to start at known coupling points and work toward higher and lower wavelengths from this starting point. The other difficulty was in finding an appropriate tolerance for the returned eigenfrequency, an appropriate $\Delta\lambda_0$ and an appropriate shift value for n_{eff}. If $\Delta\lambda_0$ was set too high the inaccuracy of the next guess would cause the program to perform to many iterations per

step, but if it were too low then procedure would have too many iterations to perform thus increasing the time again. If the tolerance was set to high for the eigenfrequency, the mode might lock onto a different mode at or near a crossing point and the accuracy would be very poor. If it were too small it may lose the mode as it would be missed if the corresponding shift value for n_{eff} was set too high. In the end, the simulation worked best when shifting n_{eff} by .0001 with $\Delta\lambda_0$=2 nm, and an eigenfrequency tolerance of .1 nm (difference between the wavelength being tested and the wavelength corresponding to the returned eigenfrequency in vacuum).

As a proof that this method produces results consistent with previous findings, the dispersion curves calculated using the solution to the case of a planar gold film as presented in [1] are recreated with the iterative approach presented above. The results, displayed in fugure 6, exhibit only a 6.8×10^{-6} MSE between the iterative solution and the analytical solution for the short range mode, and an MSE of 2.1×10^{-6} for the long range.

For the LOD optimization, only slit widths of 20 nm were used with varying gold film thicknesses, TeflonAF thicknesses, incident angles and grating pitches. A 20 nm gap was chosen as it is the thinnest gap width that can be fabricated consistently with the facilities available. Thin gaps are desired ashigher field enhancement occurs in the slit for small gaps, and the reflectivity spectra contained thin, deep resonance dips for low aspect ratios at this gap width. This by no means rules out the usefulness of other gap dimensions, but such an optimazation search was seen as beyond the scope of this work.

The dispersion curve of a sensor with a gold thickness of 52 nm, a Teflon thickness of 450 nm and a slit period of 160 nm is plotted in figure 3.2.

Only two modes were found to cross the region of the plot that describes the incident dispersion from $\theta = 60° - 65°$, no angles beyond which were used for any of the LOD calculations. This is consistent with the reflectivity results, which typically exhibit two resonance dips over the same region. Even further, the dispersion curve presents a good means of approximating reflectivity dip locations. For an incident angle of 65° using the material properties as for the dispersion curve the predicted mode minima come to 646 nm and 758 nm respectively. The reflectivity found using rigorous coupled wave theorem (RCWT) (see the next section for a more detailed discussion on RCWT) to simulate the sensor as seen in figure 3.2b shows resonance dips at 645 nm and 745 nm respectively, each having less than a 2% difference from the predicted value.

Interestingly, while tracking the mode profiles with wavelength, one will notice that in the region marked "switching region", the profiles of each mode switch, mode 1 going from symmetric to anti-symmetric, mode 2 going from anti-symmetric to symmetric. From this point mode 1 remains anti-symmetric and keeps a profile that is weighted more toward the Teflon layer. Mode 2 on the other hand gradually changes from a mode tightly confined to the slit, to a symmetric mode that reaches a large distance into the analyte at higher wavelengths.

To produce plots of H_y throughout the structure, harmonic propogation analysis was performed using Comsol with Matlab. By replacing the bottom PML in the structure used for the iterative mode search with a matched boundary with a magnetic field source,

it was possible to simulate the fields inside of the structure when illuminated with a plane wave of angle θ and $|H_{incident}| = 1$. To ensure that the harmonic propogation analysis was using the appropriate angle and wavelength to excite a plasmon mode, they were both determined by using wavelengths of minima in the reflection spectrum of the sensor modeled with RCWT at a given incident angle. Figure 3.3 plots the mode profile of H_y across x and z for modes 1 and 2 at an angle of $65°$, and figure 3.4 provides cross section plots of $|H_y|$ across key regions at the same incident angle.

In examining figure 3.4, note how the modes now present an interesting profile along the x direction at various heights in the film, while in the z direction the profile differences remain very similar to that of a planar dual mode sensor. Imagining a film that binds on the surface of the gold (ignoring the vertical sidewalls of the slit), it would be ideal to have the "surface sensitive" mode peak at the bottom of the film in the slit, and have a minimum in the slit at the top of the film. Just the opposite, it would be ideal to have the "background sensitive" mode have the opposite profile thus making the two modes more orthogonal in sensitivity. While this work has not examined the details of how to make this happen, it would be a key area of interest for future work with nano-gap enhanced SPR sensors.

While not explored in this work, it should be pointed out for that since nano-gap enhanced SPR sensors support modes that have differing sensitivities both inside and outside of the gap, it is possible to create two scenarios for the detection of surface layer binding.

1) The entire sensor surface is functionalized with receptor molecules so that a certain chemical will bind strongly the regions inside and outside of the gap.
2) Only a particular region is functionalized with receptor molecules (perhaps only inside of the gap or only outside of the gap) so that the sensor can differentiate between specific binding (high concentration on the functionalized surface, very low to negligible concentration on the non-functionalized surface) and non-specific binding (binding of molecules that aren't of interest, assumed to be low concentration on the entire surface).

The first scenario is not capable of differentiating between specific and non-specific binding under the assumption that the resonance wavelengths demonstrate a linear response to concentration changes just at the surface. Thus, even with multiple modes, the sensitivity vector for specific and non-specific binding would be near scalar multiples of one another making for a poor sensor.

Design With Optimal LOD for 20 nm Slits

A full optimization of an SPR sensor containing periodic nano-gaps is considerably harder than the optimation of planar dual-mode sensors. For the case of a planar gold film, there are already three free parameters to optimize for: incident angle, gold thickness and Teflon thickness. The nano-gaps add two more free parameters: gap period and gap width. This is coupled with the fact that the RCWT simulation process for determining reflectivity with the nano-gaps takes considerably longer than the Fresnel reflection equations used in the planar case for each sensor design. As mentioned earlier, smaller gap widths lead to higher field enhancement and thin, deep modes at low aspect

ratios. A fixed gap width of 20 nm was chosen for the sake of time, and it was determined to be the smallest gap width possible to consistently fabricate.

RCWT was chcosen as the simulation method of choice as it provides a means of accurately determining reflectivity spectrum for periodic features much less than the wavelength of light being simulated.[11] By simplifying the boundary conditions of Maxwells equations with the assumption that the structures simulated are invariant in y, and that they are only comprised of n stratified medium layers containing at most two alternating indices with a fixed periodicity, it is able to significantly reduce the calculation time for determining reflectivity when compared to other methods such as finite element analysis without losing any accuracy.

The code used to perform the RCWT calculations was taken directly from open source matlab code for Optiscan (a set of optical simulation tools) released by the lab of Tom D. Milster at the University of Arizona. By using 20 diffracted orders to calculate each solution, it was possible to check the validity of the simulation results by testing it against the Fresnel equations for the case of a planar dual mode SPR sensor. Taking the reflectivity using the Fresnel equations and RCWT from 400 to 1000 nm at a 1 nm sample width for a sensor with 52 nm of gold, 400 nm of Teflon incident at 65.5 degrees in BK7 with an analyte solution of water using the same optical properties as used with the dispersion curve analysis, the MSE between the two results was found to be only 1.765×10^{-5} demonstrating the validity of the RCWT results.

The comparison sensor of choice for the optimization was taken from [10] as the analysis used was identical to that used in this work. Using the exact data from [10] for

the spectral density of the source and detector, taken from a halogen white light source (Ocean Optics DH-2000 with deuterium source disabled) directly input to an Ocean Optics HR-4000 spectrometer, it was possible to achieve a direct comparison to the work presented there. Figure 3.5 plots the normalized spectral density used as a function of wavelength. Note the high noise at larger values of intensity distinctive of Poisson noise.

For the LOD calculations, equation (2.6) was employed with $n_d(\lambda_j)$ taken to be $S.D._{norm}(\lambda_j) * \Delta\lambda$, where $S.D._{norm}(\lambda_j)$ is the normalized spectral density interpolated at λ_j using a cubic polynomial fit, and $\Delta\lambda$ is taken here to be the distance between wavelength samples in nm. It should be noted that an LOD taken using the above value for $n_d(\lambda_j)$ produces results that are multiplied by $P_{peak}^{1/2}$, meaning that the true value of LOD is still dependant on the peak intensity of the source times the detector efficiency. This notation was used as it enables one to accurately compare the LOD of two sensors with differing spectral widths as the normalization constant is independent of the spectral width sampled. This is the only major difference from [10] where the total number of photons detected, a spectral dependent value, was used for normalization.

As with the planar dual mode optimization, a uniform index layer is assumed to bind to the surface of the gold film and at the base of the nano-gaps 1 nm thick with an index of 1.45 (see figure 3.6) for surface sensitivity determination. The background is assumed to have a uniform spectral shift of .0005 refractive index units (RIU) for background sensitivity determination. For the case of the nano-gap enhanced sensor design, it is assumed that the film only binds to the base of the slit and the top of the gold film. While in real situations this may be difficult to accomplish, due to the RCWT

simulation limitations it was impossible to simulate layers with three different indices of refraction. It is difficult to say whether or not binding on the sidewalls is indeed negligible in practice, but for a basic improvement comparison the model presented should be sufficient to show whether or not nano-gap sensors truly do provide any significant enhancement to planar SPR sensors.

In order to cut down on the simulation time, the sampling width was changed slightly from [10] to be 2 nm per sample as opposed to 1 nm per sample. For each LOD calculation the spectrum was first calculated using RCWT for a wavelength range at the given wavelength sampling rate (being 2 nm per sample here). Material properties were taken from the same sources as with the dispersion calculations using the same interpolation scheme. The derivative of the reflectivity was taken numerically. To determine the rough locations of minima and bounds for integration in determining individual mode variances using equation (2.6), a search algorithm was written in matlab to observe changes in slope. The left most minimum was taken to be the lowest wavelength sampled. If a minum below a threshold reflectivity of 0.75 was found it was considered a mode, and the next maximum was determined to be the right bound of this mode and the left bound of the next. This process was continued across the spectrum until the last mode was found, setting its right bound to the largest wavelength sampled. If an insufficient number of modes (less than 2 in our case) were found, LOD determination was abandoned as not enough data was present to calculate the LOD for both surface layer and background perturbation occurrences.

To populate the sensitivity matrix, the minimum of the reflectivity spectrum returned by the RCWT calculations was determined more accurately using the matlab

function fminbnd over a wavelength range of 60 nm around the minimum value found for that mode in the bounds/minima search algorithm described above. This value was retaken after the addition of the surface layer and then the addition of the background index shift for sensitivity evaluation. In rare occasions fminbnd would lock onto the wrong minimum value after a perturbation due to ripples in the reflectivity spectrum causing a spurious shift in wavelength before and after the perturbation, thus giving a bad sensitivity and LOD value. These would appear as sudden changes in LOD for a small change in a sensor parameter and could be discarded by further checking the LOD in that region by changing the fminbnd bounds values and seeing if the values compare.

Using the above method, LODs found for the optimal planar film sensor with a 2 nm sample grid came be 49.0844 $nm * P_{peak}^{1/2}$ for a bound layer and .0309 $RIU * P_{peak}^{1/2}$ for the uniform background index change, each value having roughly a 3% difference between the LODs for a 1nm sample grid. This is consistent with the findings of [9] that there is only a weak dependence on sample grid spacing of the peak shift estimation variance for fine enough sample grids.

To perform an LOD search, the LOD algorithm above was iterated for ranges of sensor parameters. The LODs for both surface layer binding and background index shift were stored for each sensor parameter setting and analyzed by finding the minima of each for the range of Teflon thicknesses and gold thicknesses at each incident angle and gap period sampled. The LOD search was performed through the values presented in table 4.1 for the case of a 20 nm gap width. Having lower valued dispersion curves with modes extending further into the Teflon film, the search algorithm was performed for lower

angles and slightly higher Teflon thicknesses than the search presented in [10] for comparable gold film thicknesses.

Table 3.1: LOD Optimization Searched Parameters	
Incident Angle	62° - 63.5° by .5°
Gap Period	100 nm – 220 nm by 30 nm
Teflon Thickness	450 nm – 700 nm by 50 nm
Gold Thickness	36 nm – 54 nm by 3 nm

As it was impractical to attempt to find a region where the best layer and background LOD perfectly overlap, and due to the fact that most SPR sensors are designed specifically to monitor surface binding, an emphasis was placed on finding the region of best layer LOD not far from a background LOD minimum. The region of best layer LOD in the range of searched values given in table 4.1 was found at an incident angle of 62.5° and a gap period of 160 nm. While other regions contained lower minimum values for the layer LOD than 10.23 $nm * P_{peak}^{1/2}$ found in this region, they either corresponded poorly with the background LOD values or exhibited very small ranges of sensor parameters that could be used to achieve LOD values near the minimum. The checkerboard plot of surface layer LOD and background layer LOD as a function of Teflon thickness and gold thickness is presented in figure 3.7 for the minimum region selected. While they do not perfectly overlap, note that the minimal values for background and layer LOD are closely placed making it easier to compromise between a sensor with optimal layer or background LOD.

Of the sampled values in this region, the optimal parameters for the best surface layer LOD and near minimal background LOD were found to be a gold thickness of 39 nm and a Teflon thickness of 575 nm. The referenced reflectivity of this sensor is presented in figure 3.8, having a surface layer LOD of 10.2300 $nm * P_{peak}^{1/2}$ and a background LOD of .005874 $RIU * P_{peak}^{1/2}$. These values are less than the planar film optimal values by a factor of 4.79 and 5.265 respectively.

To analyze why the nano-gap enhanced sensor with a gap width of 20 nm improved upon the performance of the planar film sensor one can examine the sensitivity matrix and the angles between the sensitivity vectors for both designs.

Planar Optimal $\mathbf{S} = \begin{bmatrix} 0.9204 & 1{,}245.6\, nm/RIU \\ 3.0304 & 5{,}770.2\, nm/RIU \end{bmatrix}, \ \theta_{sens} = 4.69°$

Nano-Gap Optimal $\mathbf{S} = \begin{bmatrix} .7286 & 67.3448\, nm/RIU \\ 4.1783 & 11{,}419\, nm/RIU \end{bmatrix}, \ \theta_{sens} = 9.5544°$

Note that, while the overall sensitivities are better for the second mode in the nano-gap enhanced sensor, the first mode has a much lower sensitivity to background index changes. This leads to greater orthogonality between the sensitivity vectors, as seen by the greater value of θ_{sens}. This greater orthogonality coupled with higher sensitivity values for the second mode make the denominator in (2.3) much larger ($|\mathbf{S}_n|^2|\mathbf{S}_t|^2 - (\mathbf{S}_n \cdot \mathbf{S}_t)^2 = 6.46 \times 10^7$ for the nano-gap enhanced sensor compared to 2.56×10^6 for the optimal planar film sensor). In the end it seems that the denominator of (2.3) (i.e. the determinant of $|\mathbf{S}'\mathbf{S}|$) is the dominant figure of merit for minimal LOD with the nano-

gap enhanced sensors presented here as the minimum variances for each mode are no more than a factor of two different between the planar optimal and the nano-gap sensor design presented. It should be noted that this value is closely related to the cross-sensitivity metric used with dual mode sensors [6], but is easily applicable to more than just two modes.

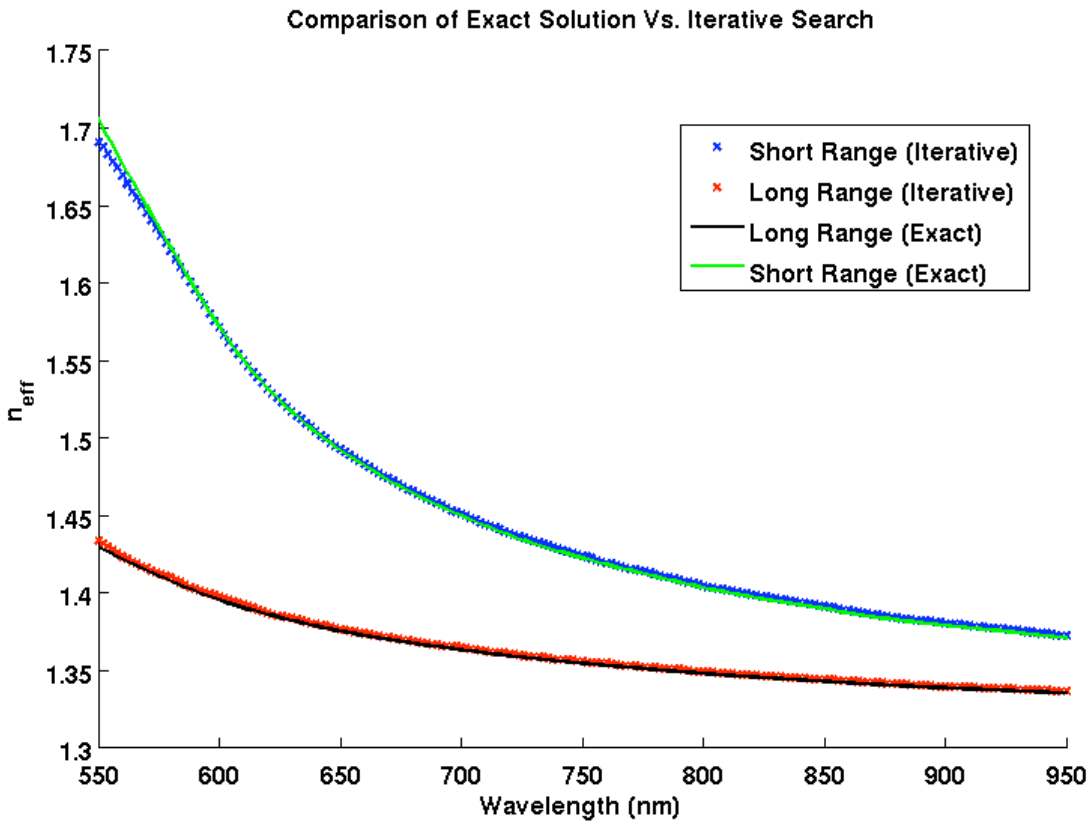

Figure 3.1 – Comparison Between Exact and Iterative Search. Comparison of exact solution and iterative determination of the effective index of both the long and short range mode in a planar dual mode sensor with infinite Teflon thickness, 52 nm of gold and an infinite water analyte.

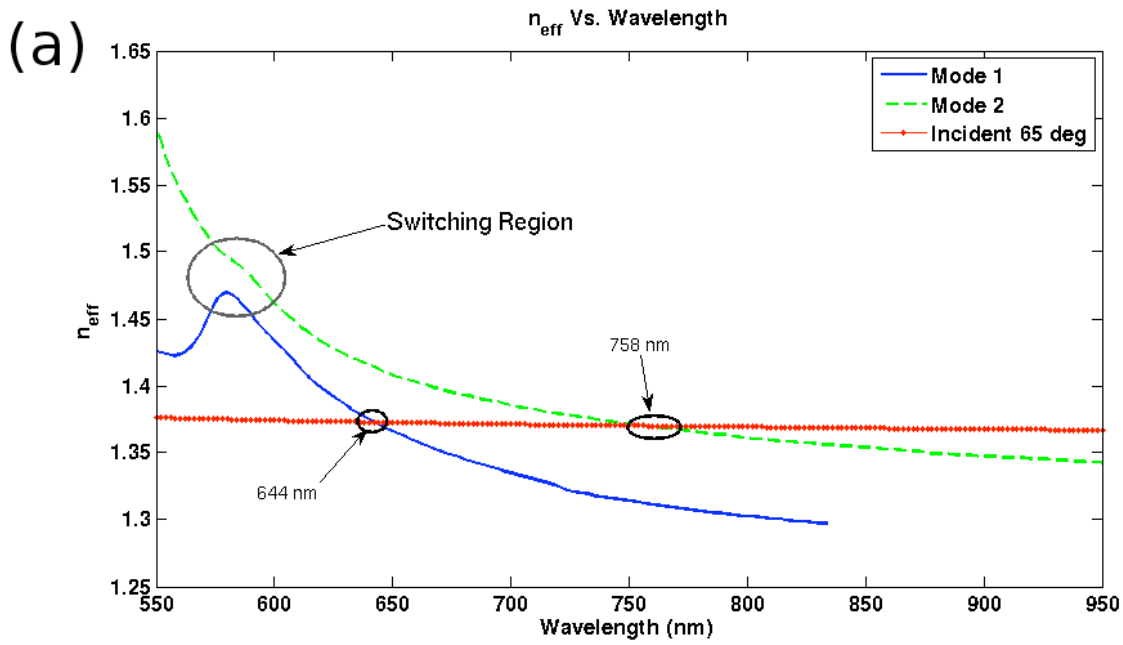

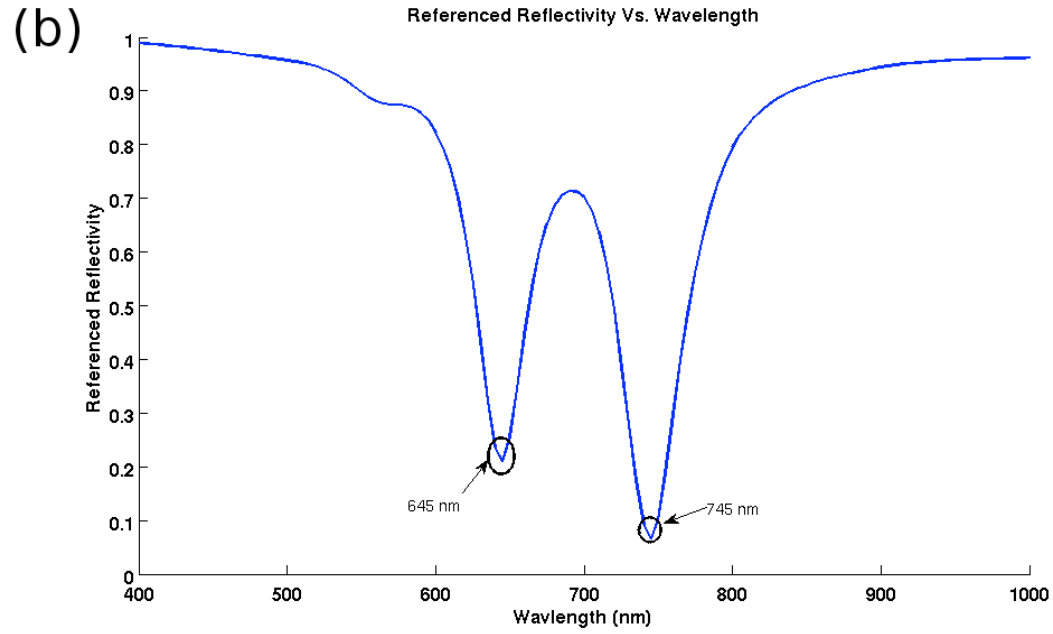

Figure 3.2 – Dispersion Curve and Reflectivity for 20nm Gaps. (a) Dispersion curve determined for a nano-gap based sensor having gaps of 20 nm, a gold thickness of 52 nm, a Teflon thickness of 450 nm a gap period of 160 nm and a water analyte. The red line represents the dispersion of the incident light in glass at an angle of 65 degrees. (b) Referenced reflectivity for the same sensor design at an angle of 65 degrees calculated using RCWT.

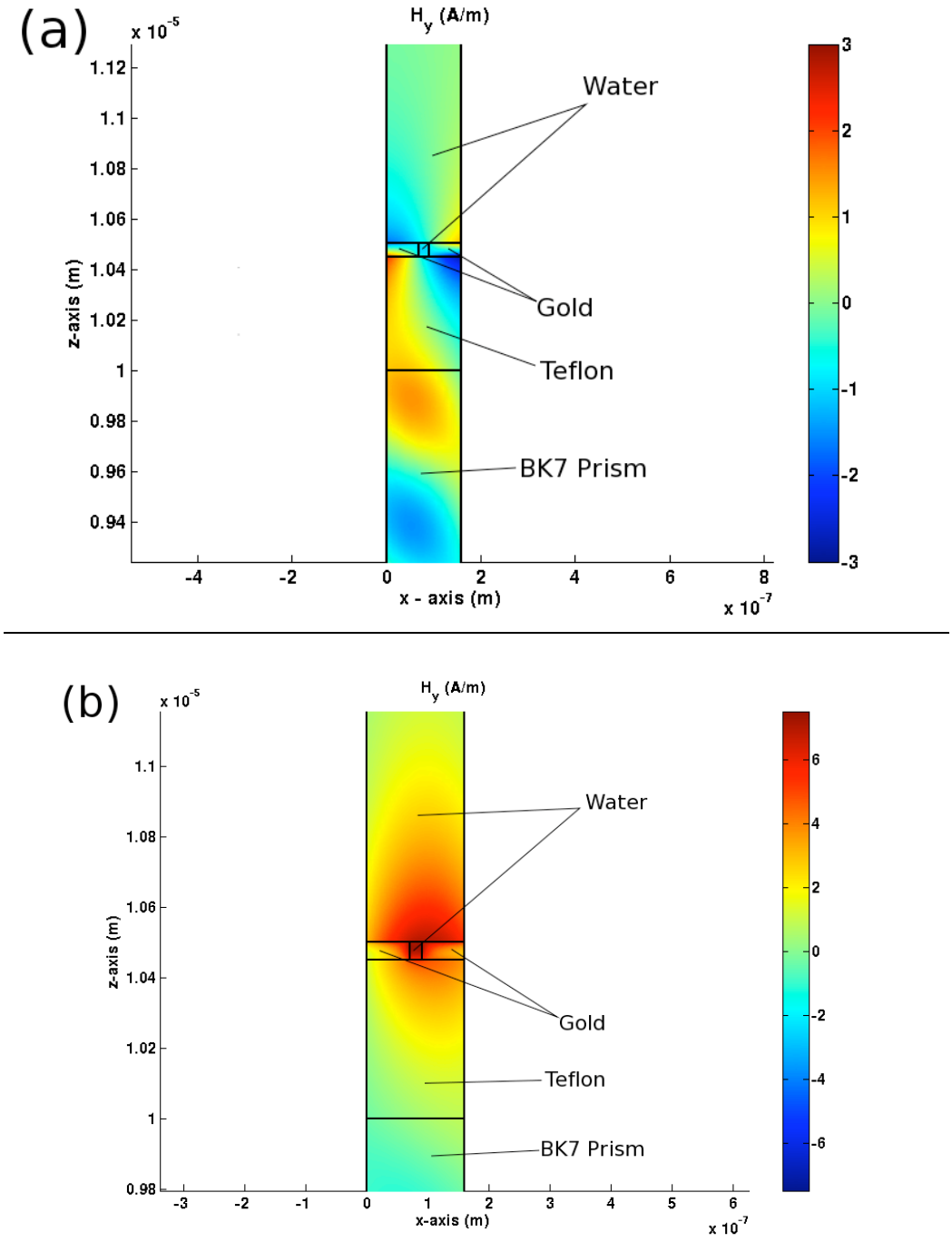

Figure 3.3 - Nano-Gap Mode Magnetic Field Profiles. Two dimensional field profiles of H_y around the slits for (a) mode 1 (anti-symmetric) and (b) mode 2 (symmetric).

(a)

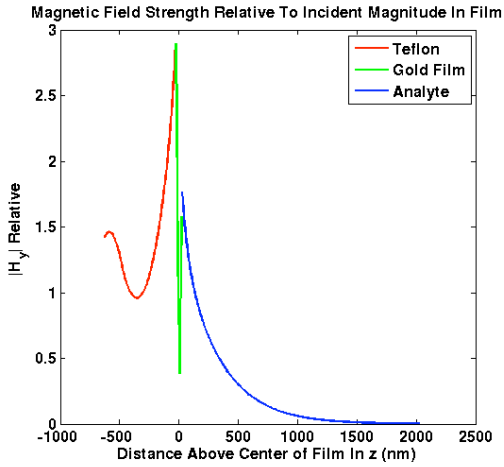
Magnetic Field Strength Relative To Incident Magnitude In Film
Teflon
Gold Film
Analyte
|H_y| Relative
Distance Above Center of Film In z (nm)

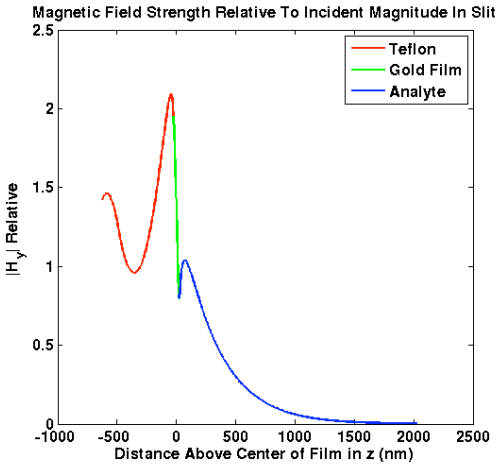
Magnetic Field Strength Relative To Incident Magnitude In Slit
Teflon
Gold Film
Analyte
|H_y| Relative
Distance Above Center of Film in z (nm)

(b)

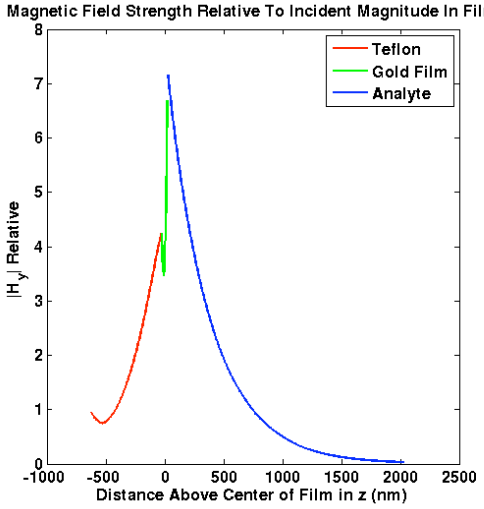
Magnetic Field Strength Relative To Incident Magnitude In Film
Teflon
Gold Film
Analyte
|H_y| Relative
Distance Above Center of Film in z (nm)

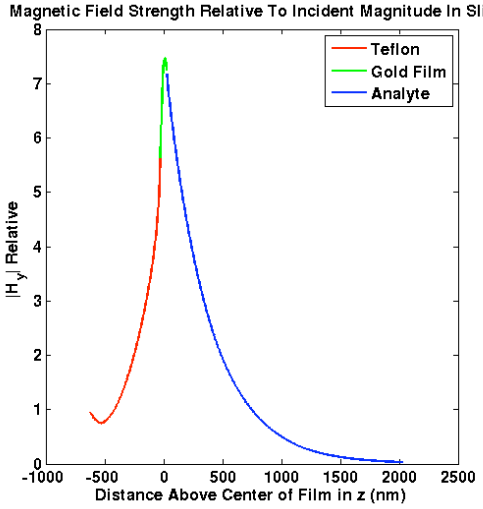
Magnetic Field Strength Relative To Incident Magnitude In Slit
Teflon
Gold Film
Analyte
|H_y| Relative
Distance Above Center of Film in z (nm)

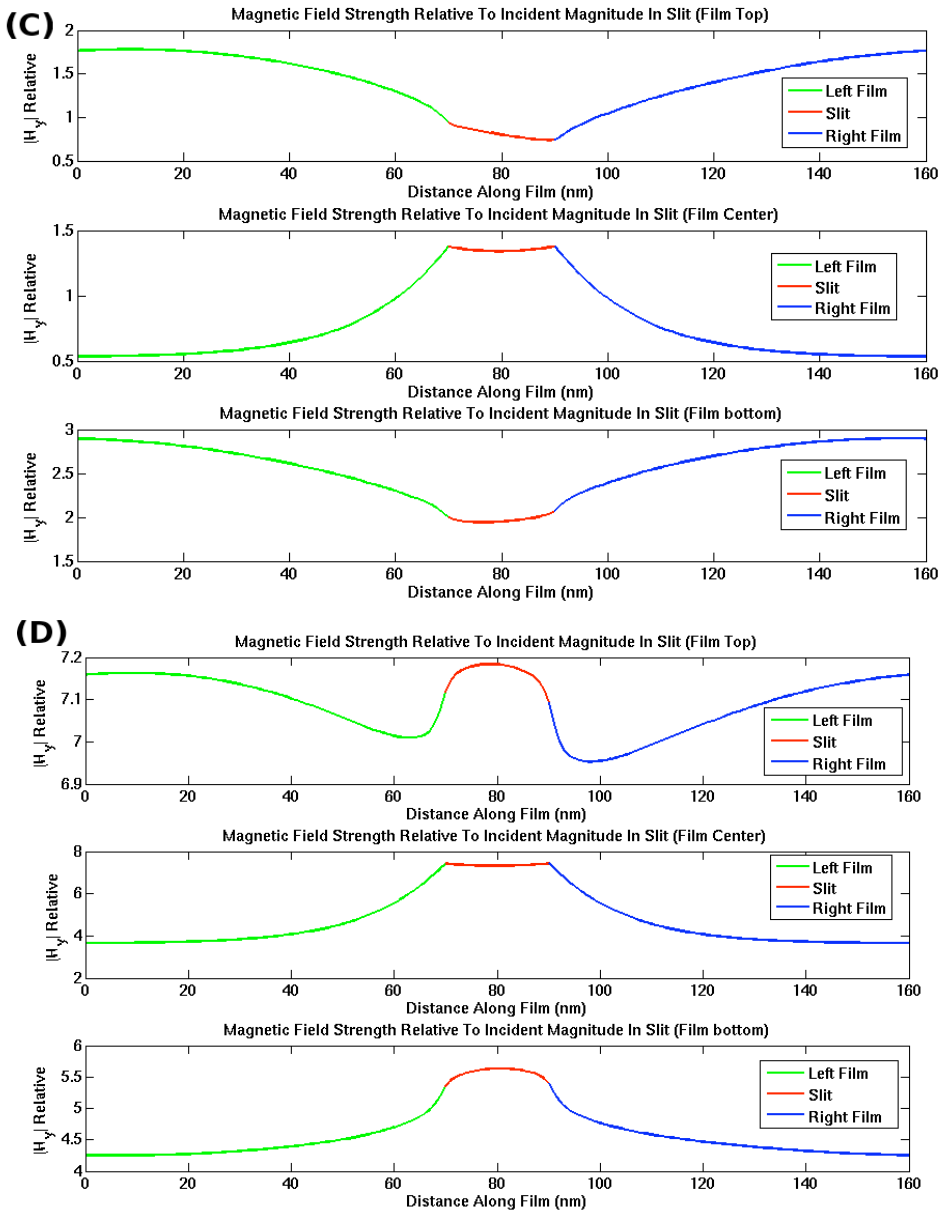

Figure 3.4 – Nano-Gap Mode Magnetic Field Cross Section Plots. (a) & (b) Vertical cross sections of modes 1 and 2 respectively both through the slit and through the film. (c) & (d) Horizontal cross sections of modes 1 and 2 respectively through the top of the film, the middle of the film and the bottom of the film.

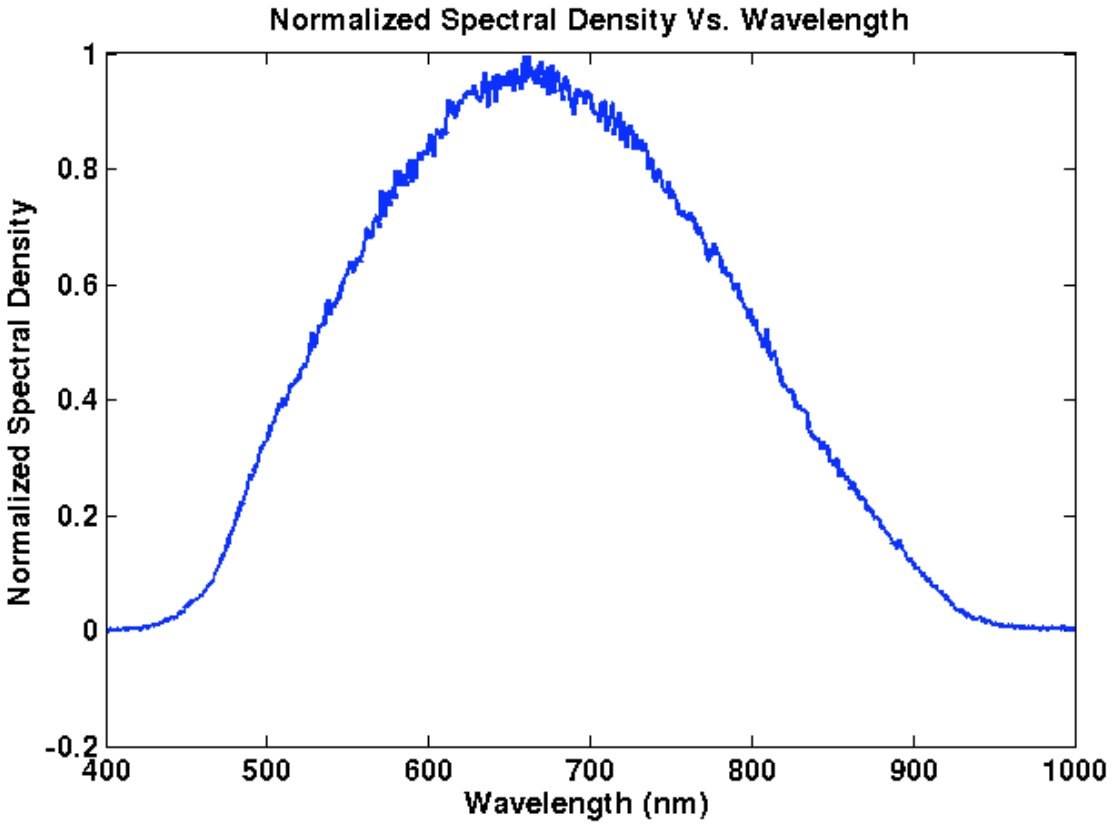

Figure 3.5 – Normalized Spectral Density of Source and Detector. This was the spectral density used for LOD calculations. The data was gathered by directly inputting a halogen white light source (Ocean Optics DH-2000 with deuterium source disabled) to an Ocean Optics HR-4000 spectrometer,

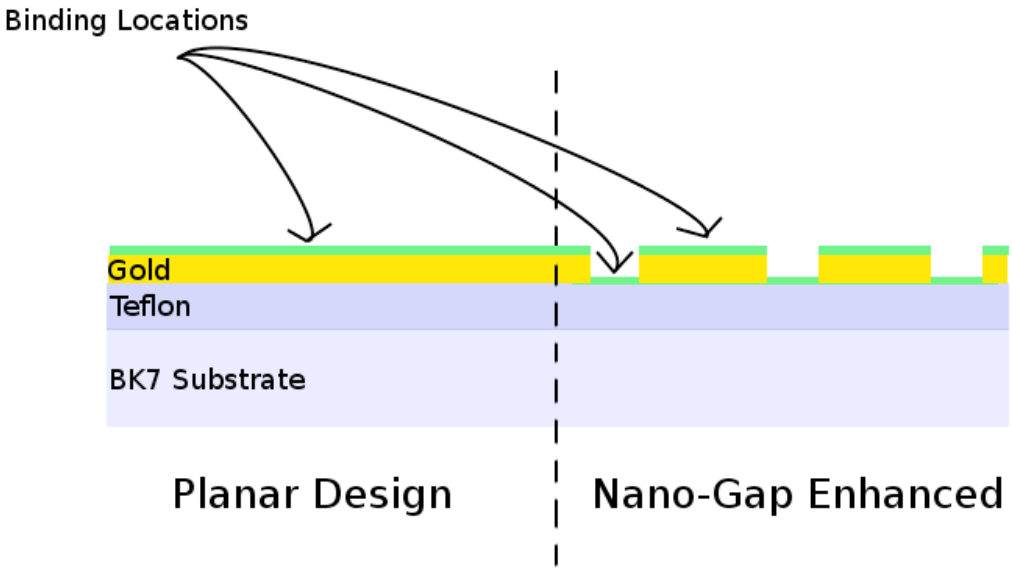

Figure 3.6 – Binding Sites With and Without Gaps. A diagram showing binding site locations simulated with both the planar design and the nano-gap enhanced design. Due to RCWT limitations, it was not possible to simulate binding on the sidewalls of the gaps.

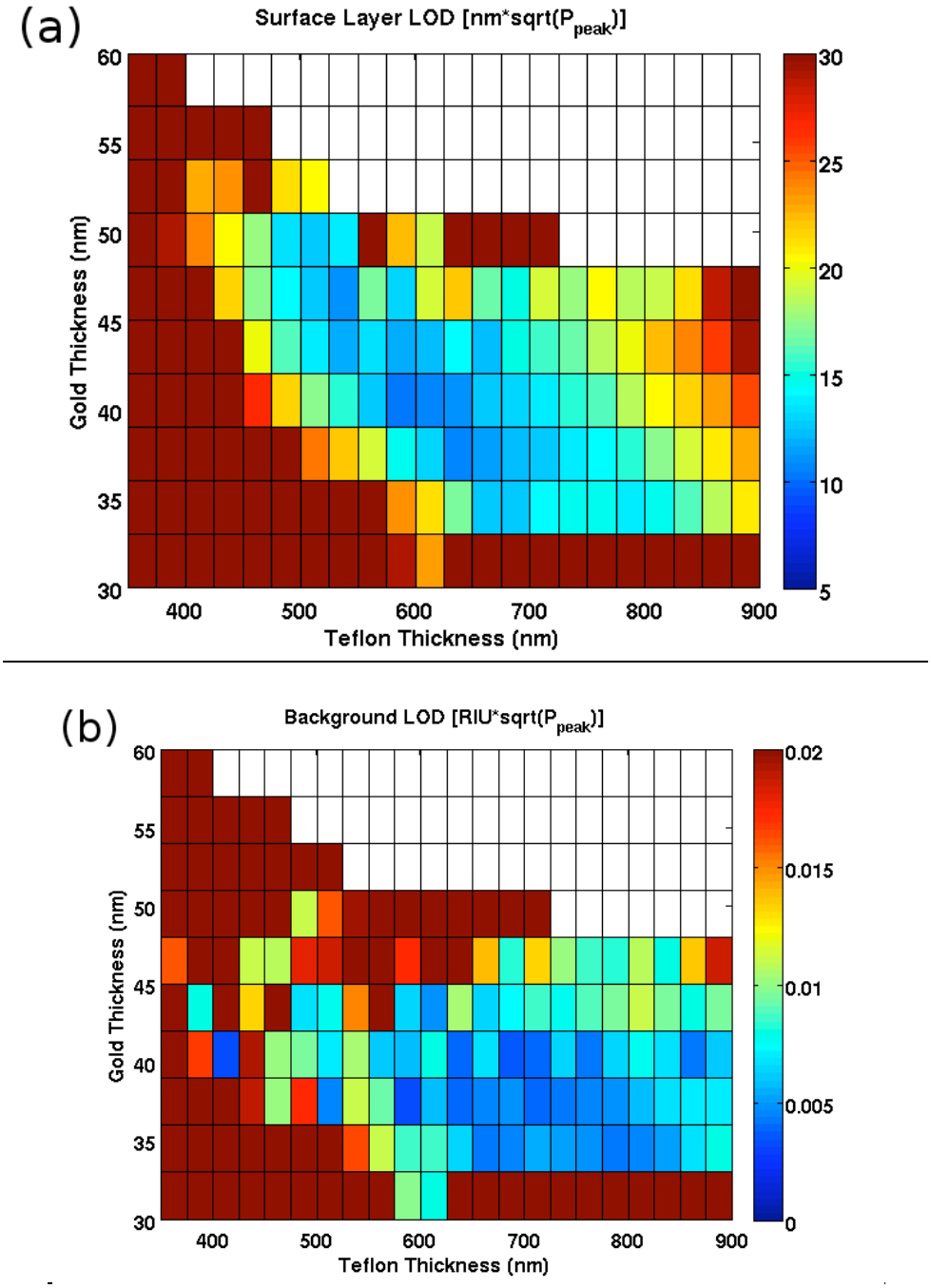

Figure 3.7 – LOD Optimal Search Results. This is a 2d checkerboard plot of LOD values at a gap period of 160 nm, a gap width of 20 nm and an incident angle of 62.5 degrees with varying gold and Teflon thicknesses for (a) surface LOD and (b) background LOD. The white regions are where on or both of the modes were not beyond the threshold and it was impossible to calculate LOD. The data taken in the original sample was expanded for plotting purposes.

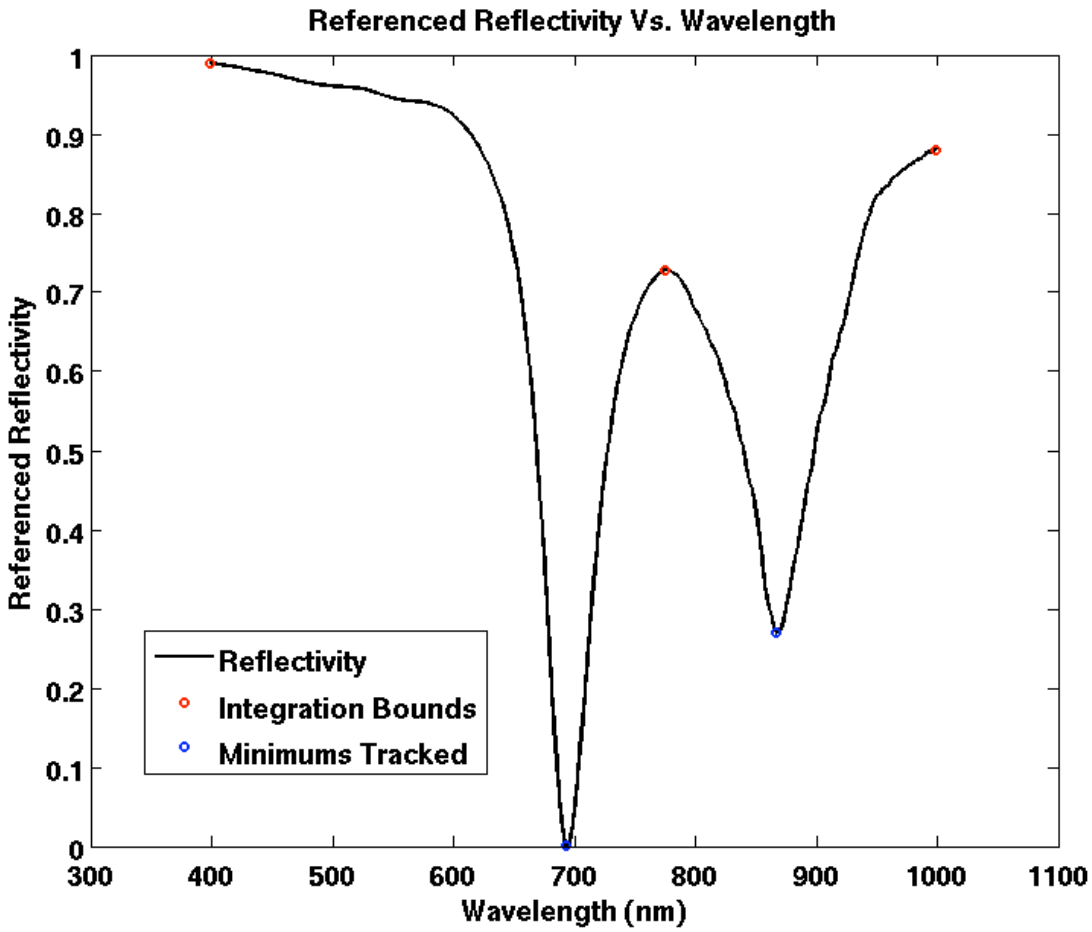

Figure 3.8 – Optimal Design Reflectivity. Referenced reflectivity plot of sensor design having optimal layer LOD. The integration bounds and rough minima found are shown to demonstrate where the variance integrals were taken for LOD calculations.

Chapter 4: Fabrication and Testing

As with any device, theoretical optimization is considerably devalued if one cannot fabricate a structure that closely matches simulation. While it was not the intent of this project to come away with a perfectly fabricated version of the optimal sensor design, it was deemed important to show that the fabrication techniques for making nano-gap enhanced sensors similar to those proposed are within the realm of possibility.

With minimum feature sizes of 20nm, e-beam lithography was chosen as the method for writing the nano-gap features. However, this influenced the choice of substrate, as a purely insulating substrate will result in charging thus affecting the write procedure. To work around this problem, a BK7 glass slide coated with a thin film of indium tin oxide (ITO) manufactured by SPI supplies was used as the substrate. The ITO film was measured to be roughly 123 nm thick by using spectroscopic ellipsometry. Before continuing the fabrication procedure, the sensor design to be created (a Teflon thickness of 500nm, gold thickness of 45nm a gap period of 160nm and a slit width of 20nm) was simulated for an incident angle of 63° to ensure that the ITO film would not perturb the modes enough to significantly alter reflectivity spectrum. The results, plotted in figure 4.1, demonstrated that the ITO film present should only slightly alter the spectrum.

A standard spin-coating procedure was used to achieve a thin film of Teflon close to 500nm. A fluorosilane adhesion promoter (Lancaster Synthesis, Inc.) was first applied to the ITO coated glass slide to increase Teflon adhesion to the surface. Teflon-AF 1600 (Dupont, Inc.) diluted with Fluorinert FC-40 (3M) was then spun onto the

treated substrate ate a rate of 2800 rpm for 30 seconds. The subsequent Teflon film was measured to be 524 nm thick using spectroscopic ellipsometry. This sensor was then treated in oxygen plasma for one minute and thirty seconds using a microwave plasma etcher (Plasma-Preen, Model II-862). After the etching the Teflon thickness was reduced to 492nm.

For this process HSQ, a negative e-beam resist, was chosen as it has been demonstrated that pillars close to 20nm wide can be fabricated by exposing the resist to single pixel e-beam lines. Using HSQ also reduces the exposure area since only the gap regions needed to be exposed. However, in order to achieve a properly spin-coated thin film of HSQ on Teflon, it was necessary to sputter-coat the Teflon with a very thin layer of titanium (~2-5nm) to improve adhesion. After this process, ellipsometry provided thickness measurements of 123.5nm ITO, 420nm Teflon and 6nm of titanium. The results were trusted as the ITO thickness was consistent with earlier readings, and it was reasoned that the plasma exposure during the two-minute pre-sputter process etched the Teflon film, similar to the oxygen plasma exposure. After spin-coating, the HSQ film thickness was measured to be approximately 89nm using spectroscopic ellipsometry.

The nano-gap pattern was written near the middle of the sample (Raith, Model: e-Line) over a 2mm x 3mm area. The pattern was then developed using Microposit MF319 Developer (Shipley). After this procedure only the thin lines of HSQ, presumably the width of the slits, were remaining (see figure 4.2 for a flow chart of the patterning, development, coating and liftoff process). This pattern was then sputter-coated with a thin film of gold measured to be approximately 48 nm thick using

spectroscopic ellipsometry. To remove the HSQ, the pattern was treated with a 1:100 HF to DI water solution for one minute which completed the fabrication process.

Subsequent analysis using scanning electron microscopy (SEM) revealed both positive and negative results. Figure 4.3 shows several images taken with the sample tilted at an angle of 45 degrees. It is apparent that the thin lines in the sample appear raised compared to the surrounding area. Due to the matching surface characteristics of the regions between the raised lines and the surrounding gold surface, it was reasoned that these regions are also gold. The presence of thin raised lines divided by wide regions of gold demonstrates that the liftoff procedure failed. The lines were measured to be roughly 40nm wide having a periodicity of 140nm using the SEM at various locations across the sample. On a positive note, the lines were well resolved during development, and quite uniform throughout much of the patterned area. This provides much hope that with more time and effort, one could hone the process and perfect liftoff procedures to successfully create a working nano-gap sensor.

For optical analysis, the sample was mounted onto an equilateral BK7 prism by using an index matching fluid (Cargille Laboratories). A Halogen white light source (Ocean Optics DH-2000 with deuterium source disabled) was then incident onto the sample through the prism at various angles. The reflected beam was analyzed with an Ocean Optics HR-4000 spectrometer. Using a rotating polarizer mount, TE reflection spectra were measured both on and off the patterned area and used as a reference for the respective TM reflection spectra. Figure 4.4 plots the experimental and theoretical results both on and off the pattern for various angles using both water and ethanol as analyte solutions.

With the beam off of the sample, the referenced reflectivity matched closely to the planar dual mode sensor's theoretical results, including the ITO and Ti films added in processing. For the spectra taken on the patterned area, it appears as if a mode is present for lower wavelengths as predicted by the theoretical calculations. However, the mode appears to be "washed out" on the right hand side. This is assumed to be due to effects of widening of the mode, due to inconsistencies in the pattern of nano-gaps, and also an averaging effect, due to the incident light beam falling on and off the patterned area during testing.

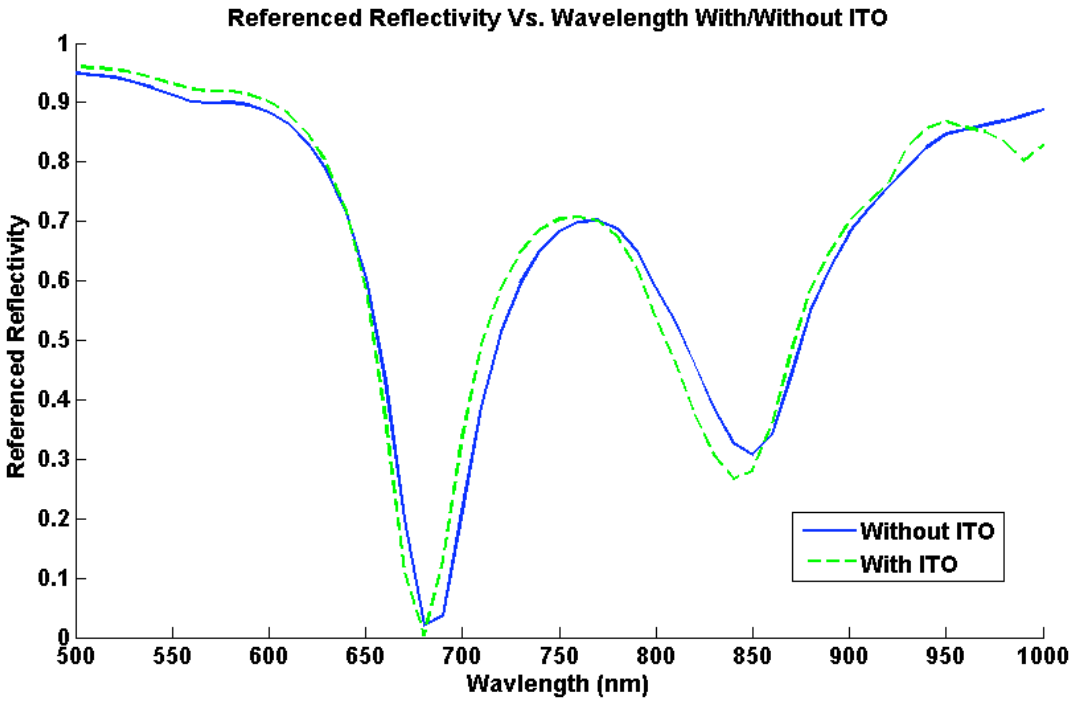

Figure 4.1 – Reflectivity Before and After ITO. Comparison of the referenced spectrum of the nano-gap enhanced sensor design proposed for fabrication both before and after the addition of ITO.

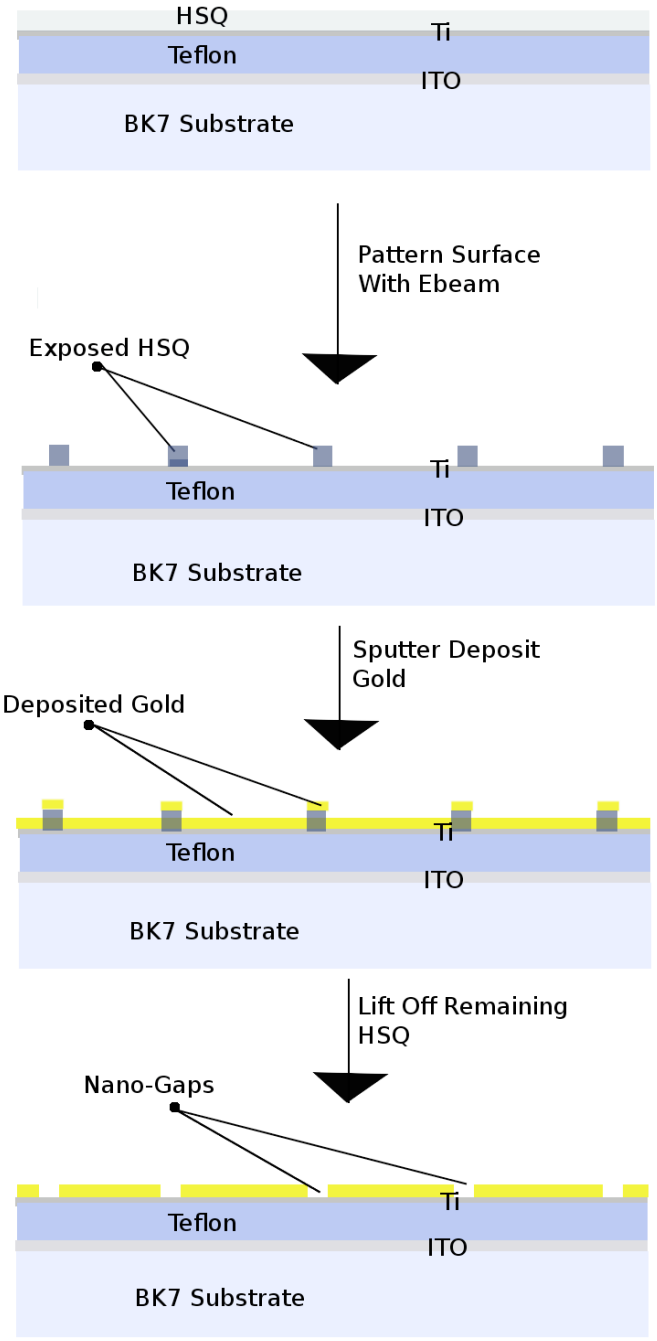

Figure 4.2 – Fabrication Procedure. Flow chart demonstrating the procedure for creating the nano-gaps after the sample is coated with HSQ.

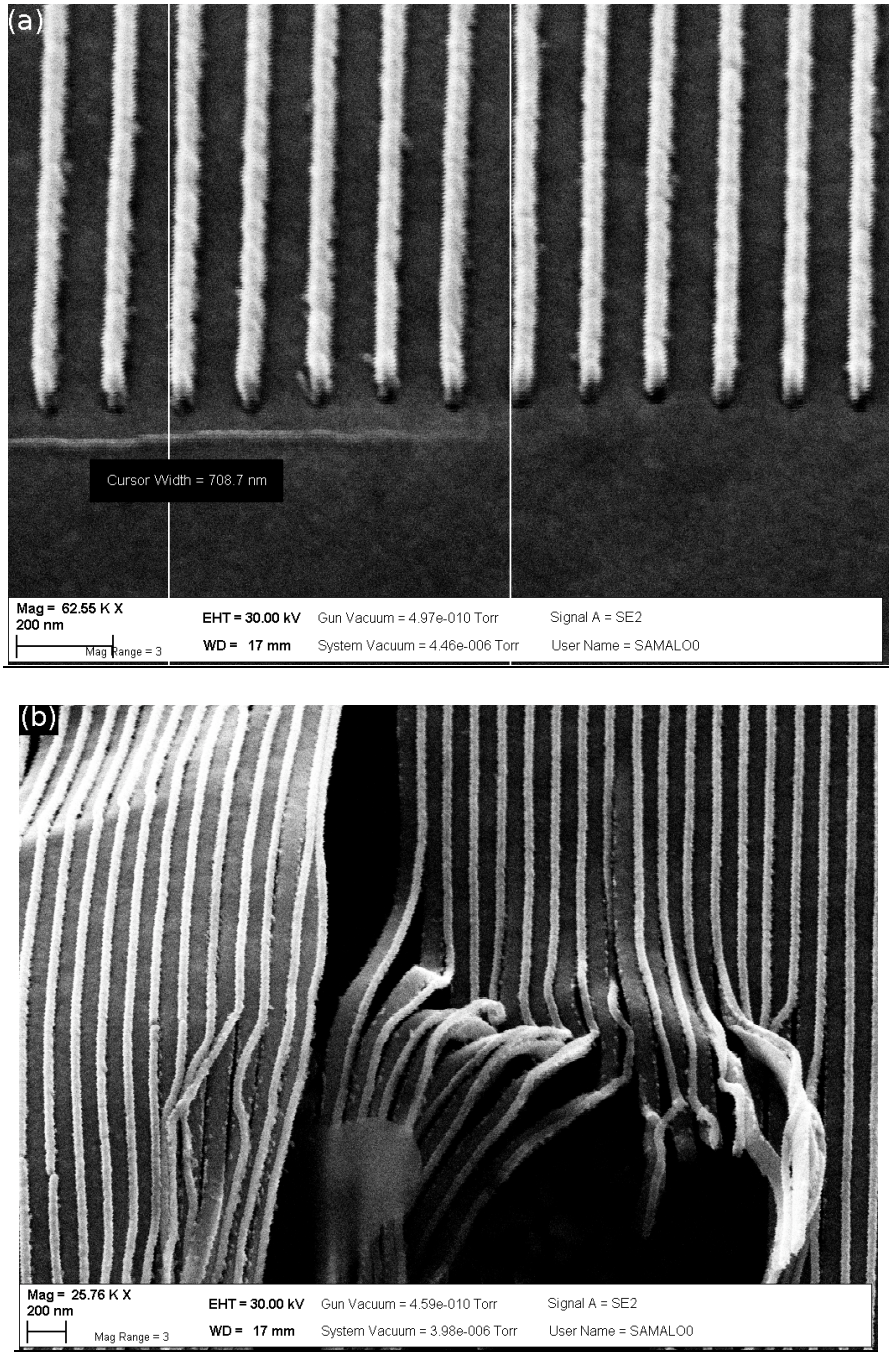

Figure 4.3 – SEM Images of Fabricated Sensor. SEM images taken with the sample tilted at 45 degrees used to demonstrate that the HSQ was not lifted off. In (a) the thinner lines appear raised on the edge not recessed. In this plot you can also see that the periodicity of the lines is around 140 nm not 160 nm as intended. For (b) the tear in the gold film, placees the thinner strips at unique angles to better demonstrate that they are indeed raised.

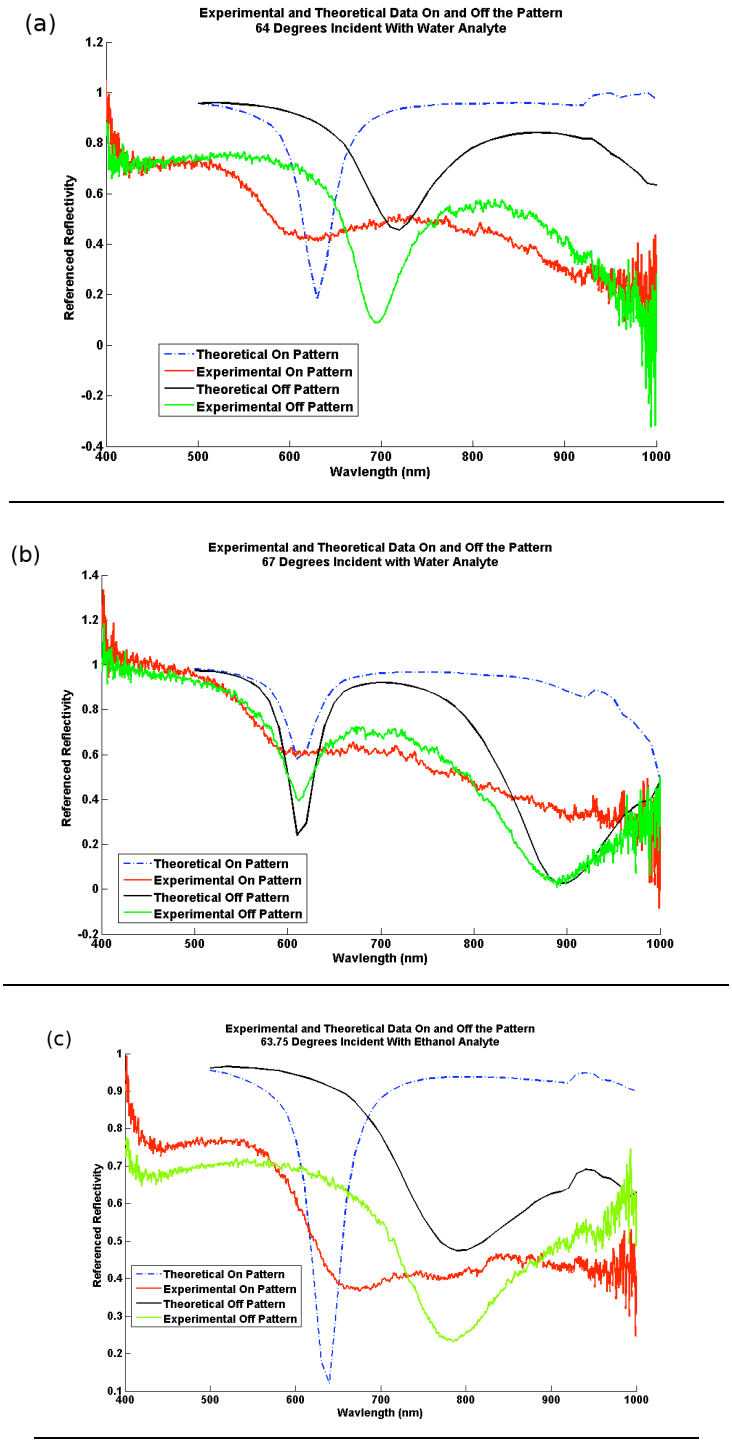

Figure 4.4 – Comparison of Experimental and Theoretical Reflectivities on and off the Pattern. Plots of experimental and theoretical referenced reflectivity both on and off the pattern for varying angles and analyte solutions. (a) 64 degrees incident, water analyte, (b) 67 degrees incident, water analyte solution, and (c) 63.75 degrees incident, ethanol analyte solution.

Chapter 5: Conclusions…Looking Ahead

It has been demonstrated through simulation that by creating a periodic array of subwavelength nano-gaps inside of the gold film of a traditional SPR sensor design it is possible to reduce both surface and backgroung LOD by approximately a factor of 5 from the optimal design presented in [10].

For the region of incident angles between 62 and 65 degrees used in this work, two modes were efficiently excited. Analysis of the dispersion curve and magnetic field profiles of each mode demonstrated that the first mode, coupled to at lower wavelengths for the case of 20nm gaps, is more confined to the film and analogous to the anti-symmetric SPR mode found with planar films. The second mode, coupled to at higher wavelengths for the case of 20nm gaps, is more gap confined and analogous to the symmetric SPR mode found with planar films. Because the second mode is more confined to the gap, especially for lower wavelengths where its fields are almost purely contained within the gap, the second mode is thought to be either a pure dielectric slab mode, or a mixture of both dielectric slab and surface modes.[12] While there is still a lot of room for improvement, this work has demonstrated how one can use the unique nature of plasmon modes within nano-gap enhanced sensors to further improve SPR sensing performance.

Through analyzing the linear equations used for determing perturbation values from the SPR sensing results and how they apply to LOD, it was found that it is just as important that the modes have orthogonal responses to perturbations as it is that they have high sensitivity vector magnitudes (the vector containing sensitivity values of every mode to a given perturbation value). While the nano-gap enhanced sensor has varying

field profiles both in x and z, traditional planar designs only allow for two coupled modes with little ability to change their electromagnetic field profiles. This makes the engineering of mode profiles to increase orthogonality quite limited in comparison to nano-gap enhanced sensors. This was directly observed when comparing the optimal design for 20nm gaps with the optimal design of a dual-mode planar design with a similar structure. While the variance of the first mode found with the nano-gap sensor had a tighter and deeper resonance dip than that of the planar design, the minimum variance of the minimum estimation for this mode was no more than a factor of two better than that of the planar design. Furthermore, the minimum variance of the minimum estimate was worse for the second mode of the nano-gap enhanced sensor. However, when comparing the sensitivity matrix, it was found that the angle between the two sensitivity vectors for the nano-gap sensor was nearly doubled (9.55° for the nano-gap sensor as opposed to 4.69° for the planar film design), and the magnitude of each sensitivity vector was increased. This lead to the denominator of the LOD equation, $|\mathbf{S}_n|^2|\mathbf{S}_t|^2 - (\mathbf{S}_n \cdot \mathbf{S}_t)^2$, to be more than an order of magnitude higher for the nano-gap enhanced sensor, therefore making it the dominant factor in LOD reduction.

One can begin to see why a nano-gap enhanced sensor presents such increased orthogonality between the sensitivity vectors by qualitatively analyzing the field profiles of the modes both in and out of the slit (see figures 3.3, 4). For a sensor with 20nm gaps, the mode profiles going into the analyte solution on top of the gold film are analogous to those of the first and second mode of the planar film design. However, over the slit, the fist mode (already having a profile more sensitive to surface changes), has a much larger peak field intensity at the location of binding (just above the Teflon film) than is

impossible to achieve with the planar design (figure 3.4b). For the second mode, the converse is true. Over the slit, the second mode (already having a profile more sensitive to background changes), has a much larger peak field intensity in the analyte solution which is once again impossible to achieve with the planar film design (figure 3.4b). Thus the first mode should be relatively more sensitive to surface changes, and the second mode relatively more sensitive to background changes when compared to the planar film design, thus increasing orthogonality. (This effect is most strongly presented in the first mode, which has a greatly reduced sensitivity to background changes, making it very interesting for applications that can only utilize a single mode). From here, future work should look into determining whether it is possible to increase this orthogonality effect by adjusting the structure parameters, including gap width. Since more than two modes are possible using the nano-gap enhanced sensor, future work should also look to utilizing them. Sensors with multiple modes provide more information for analysis, thus opening up more experimental possibilities (such as analyzing both specific and non-specific binding).

While a successful fabrication was not achieved in this work, it was found that with electron beam lithography it is possible to achieve periodic lines 40 nm wide having a 140 nm period length in HSQ. With further work, it is believed that the fabrication process and liftoff of the HSQ film is indeed possible, and that the fabrication of working nano-gap enhanced sensors is indeed within the realm of possibility giving even greater merit to the simulations presented.

Appendix A: Harmonic Analysis Code

```
%%%%%%%%%%%%%%%%%%%%%%%%%%%%%%%%%%%%%%%%%%%%%%%%%%%%%%%%%%%%%%
%%%%%%%%%%%%
%slitsModeSearch.m
%
%MATLAB function that utilizes Comsol to perform harmonic propogation
%analysis on a thin film dual-mode SPR sensor with slits.  Materials and
%structure parameters are given as inputs, with the Comsol fem data
%structure given as the output for later analysis (such as ploting mode
%profiles or creating videos).
%
%Code written by Phillip D. Keathley with automated Comsol code: Generated
%   by COMSOL 3.5a (COMSOL 3.5.0.603, $Date: 2008/12/03 17:02:19 $)
%
%Description of inputs:
%   incidentMat - incident material data file (usually the prism material)
%   matchedMat - material data file of the matched layer (usually Teflon)
%   filmMat - material data file of the plasmon supporting film
%   analyteMat - material data file of the analyte solution
%   slitMat - material data file of material in the slit
%   wavelength - wavelength of light (in vacuum) to be tested
%   theta - angle of incident light
%   gratWidth - width of one period of the structure (which is inherently a
%       grating
%   filmThick - thickness of the plasmon supporting film
%   analyteThick - thickness of the analyte material
%   matchedThick - thickness of the matched material
%   incidentThick - thickness of the incident material
%   slitWidth - width of the slit
%   pmlThick - thickness of the PML layer (at the top of the structure).
%   maxIter - maximum number of iterations to perform (applied to old
%       eigenfrequency code of same name... does not apply to this version
%       with harmonic propagation).
%
%Description of output:
%   femPlot - fem structure containing the solution
%
%Last updated: 8/6/09
%%%%%%%%%%%%%%%%%%%%%%%%%%%%%%%%%%%%%%%%%%%%%%%%%%%%%%%%%%%%%%
%%%%%%%%%%%%


function femPlot = slitsModeSearch(incidentMat, matchedMat, filmMat, analyteMat, ...
    slitMat, wavelength, theta, ...
    gratWidth, filmThick, analyteThick, matchedThick, incidentThick, slitWidth, pmlThick, ...
    maxIter);
```

```
flclear fem

% COMSOL version
clear vrsn
vrsn.name = 'COMSOL 3.5';
vrsn.ext = 'a';
vrsn.major = 0;
vrsn.build = 603;
vrsn.rcs = '$Name:  $';
vrsn.date = '$Date: 2008/12/03 17:02:19 $';
fem.version = vrsn;

% Geometry

g2=rect2(gratWidth,incidentThick,'base','corner','pos',{'0','0'},'rot','0');

g4=rect2(gratWidth,matchedThick,'base','corner','pos',{'0',incidentThick},'rot','0');

g6=rect2((gratWidth/2 - slitWidth/2) ,filmThick,'base','corner','pos',{'0',incidentThick +
matchedThick},'rot','0');

g8=rect2(slitWidth, filmThick,'base','corner','pos',{gratWidth/2 - slitWidth/2, incidentThick +
matchedThick},'rot','0');

g9=rect2((gratWidth/2 - slitWidth/2) ,filmThick,'base','corner','pos',{gratWidth/2 +
slitWidth/2,incidentThick + matchedThick},'rot','0');

g10=rect2(gratWidth, analyteThick,'base','corner','pos',{'0',incidentThick + matchedThick +
filmThick},'rot','0');

g11 = rect2(gratWidth, pmlThick, 'base', 'corner', 'pos', {'0', incidentThick + matchedThick + filmThick +
analyteThick}, 'rot', '0');

% Analyzed geometry
clear s
s.objs={g2,g4,g6,g8,g10, g9, g11};
s.name={'R1','R2','R3','R4','R5', 'R6', 'R7'};
s.tags={'g2','g4','g6','g8','g10', 'g9', 'g11'};

fem.draw=struct('s',s);
fem.geom=geomcsg(fem);

% Initialize mesh
fem.mesh=meshinit(fem, ...
                'hauto',5);

% Refine mesh
fem.mesh=meshrefine(fem, ...
```

```
                'mcase',0, ...
                'rmethod','regular');

% Refine mesh
fem.mesh=meshrefine(fem, ...
                'mcase',0, ...
                'rmethod','regular');

% % Refine mesh
% fem.mesh=meshrefine(fem, ...
%                 'mcase',0, ...
%                 'rmethod','regular');


n_incident = real(sqrt(eps_interp(incidentMat, wavelength)));

%Determine n_eff from wavelength and incoming angle.  This will be used
%with the floquet periodicity phase shift determination.
n_eff = sind(theta)*n_incident;
kf = 2*pi*n_eff/wavelength;


%%%%%%%%%%%%%%%%%%%%%%%%%%%%%%%%%%%%%%%%%%%%%%%%%%%%%%%%%%%%%%%%%%%%%%%%%%%%
%
%%Solver data for determing the modes
%%%%%%%%%%%%%%%%%%%%%%%%%%%%%%%%%%%%%%%%%%%%%%%%%%%%%%%%%%%%%%%%%%%%%%%%%%%%
%


% Application mode 1
clear appl
appl.mode.class = 'InPlaneWaves';
appl.name = 'rfwh';
appl.module = 'RF';
appl.sshape = 2;
appl.assignsuffix = '_rfwh';
clear prop
prop.field='TM';
prop.inputvar='lambda';
appl.prop = prop;


clear bnd
bnd.type = {'periodic',...
   'SC', ...
   'SC', ...
   'cont'};
%floquet periodic settings
```

```
bnd.kper = {{kf;gratWidth},...
    {0;0}, ...
    {0;0}, ...
    {0;0}};
bnd.pertype = {'floque','sym','sym','sym'};

%give the source a magnitude of H = 1
bnd.H0 = {{0;0;0},....
    {0;0;'1'},...
    {0;0;0},...
    {0;0;0}};
%Give the source a direction of theta by specifying the wavevector
%components in x and y (this defines a vector direction, where tangent of
%the two components will be taken to get the angle of incidence in the
%medium adjacent to the boundary source.  Therefore, magnitude does not
%matter, only that the x and y components specify the appropriate angle and
%direction (+/-)).
bnd.kdir = {{'-nx_rfwh';'-ny_rfwh'},{sind(theta);cosd(theta)}, {'-nx_rfwh';'-ny_rfwh'}, {'-nx_rfwh';'-
ny_rfwh'}};
bnd.srctype = {'H', 'H', 'H', 'H'};
bnd.ind = [1,2,1,4,1,4,1,4,1,4,3,4,4,4,4,4,4,1,1,1,1,1];
appl.bnd = bnd;

clear equ
equ.coordOn = {{0;0},{0;0},{0;0},{0;0},{0;1},{0,0}};
equ.n = {sqrt(eps_interp(incidentMat, wavelength)), ...
    sqrt(eps_interp(matchedMat,wavelength)), ...
    sqrt(eps_interp(filmMat, wavelength)), ...
    sqrt(eps_interp(analyteMat, wavelength)), ...
    sqrt(eps_interp(analyteMat, wavelength)), ...
    sqrt(eps_interp(slitMat, wavelength))};
equ.Stype = {'none','none','none','none','coord', 'none'};
equ.matparams = 'n';
equ.ind = [1,2,3,4,5,6,3];
appl.equ = equ;
appl.var = {'H0iz',['exp(-j*k0_rfwh*x)'], ...
  'lambda0', wavelength};
fem.appl{1} = appl;

fem.frame = {'ref'};
fem.border = 1;
clear units;
units.basesystem = 'SI';
fem.units = units;

% ODE Settings
clear ode
clear units;
```

```
units.basesystem = 'SI';
ode.units = units;
fem.ode=ode;

% Multiphysics
fem=multiphysics(fem);

% Extend mesh
fem.xmesh=meshextend(fem);

% Solve problem
fem.sol=femstatic(fem, ...
                  'complexfun','on', ...
                  'conjugate','on', ...
                  'solcomp',{'Hz'}, ...
                  'outcomp',{'Hz'}, ...
                  'blocksize','auto', ...
                  'maxiter',maxIter);


% Save current fem structure for restart purposes
fem0=fem;

femPlot = fem;
```

Appendix B: Dispersion Calculation Code

```
%%%%%%%%%%%%%%%%%%%%%%%%%%%%%%%%%%%%%%%%%%%%%%%%%%%%%%%%%%%%%%%%%%
%%%%%%%%%%%%
%dispersionCalculationSlits_adaptive.m
%
%MATLAB program utilizing COMSOL to search for physically consistent
%surface plasmon modes within a thin metal film containing a
%periodic array of slits.  By altering kx it is able to "map" the
%dispersion profile of the modes.
%
%Code written by Phillip Donald Keathley with autoimated Comsol code
%   Generated by COMSOL 3.5a (COMSOL 3.5.0.603, $Date: 2008/12/03 17:02:19)
%
%Last updated: 8/6/09
%%%%%%%%%%%%%%%%%%%%%%%%%%%%%%%%%%%%%%%%%%%%%%%%%%%%%%%%%%%%%%%%%%
%%%%%%%%%%%%

clear all;

%set the wavelength of incoming light, and wavelength increment
wavelengthStart = 596e-9;
maxWavelength = 596e-9;
waveIncrement = 2e-9;

%guess at beginning wavelength n_eff, and the previous n_eff value
n_eff_guess = 1.5809;
n_eff_previous = 1.5809;

%determine the n_eff step size to use
n_eff_step = .0001;

%Set the tolerance (in nm) for the search algorithm.
tolerance = .25e-9;

%set the incident/matched/film/analyte material files to be used
incidentMat = 'teflonaf_cauchy';
matchedMat = 'teflonaf_cauchy';
filmMat = 'gold_jc';
analyteMat = 'water_crc';
slitMat = 'gold_jc';
%Since this is technically a form of diffraction grating, set the grating
%width for the periodicity.
gratWidth = 400e-9;

%Set structure physical dimensions (all in meters)
filmThick = 52e-9;
analyteThick = 5e-6;
```

```
matchedThick = 4.5e-7;
incidentThick = 5e-6;
slitWidth = 20e-9;


%set the number of eigenvalues to find, and how many iterations to take to
%determine each eigenmode.
eigSolutions = 10;
eigIter = 300;

%The PML functionality now works, so set a PML thickness.
pmlThick = 1000e-9;

%%%%%%%%%%%%%%%%%%%%%%%%%%%%%%%%%%%%%%%%%%%%%%%%%%%%%%
%%%%%%%%%%%%%%%%%%%%
flclear fem

% COMSOL version
clear vrsn
vrsn.name = 'COMSOL 3.5';
vrsn.ext = 'a';
vrsn.major = 0;
vrsn.build = 603;
vrsn.rcs = '$Name:  $';
vrsn.date = '$Date: 2008/12/03 17:02:19 $';
fem.version = vrsn;

% Geometry

g2=rect2(gratWidth,incidentThick,'base','corner','pos',{'0','0'},'rot','0');

g4=rect2(gratWidth,matchedThick,'base','corner','pos',{'0',incidentThick},'rot','0');

g6=rect2((gratWidth/2 - slitWidth/2) ,filmThick,'base','corner','pos',{'0',incidentThick +
matchedThick},'rot','0');

g8=rect2(slitWidth, filmThick,'base','corner','pos',{gratWidth/2 - slitWidth/2, incidentThick +
matchedThick},'rot','0');

g9=rect2((gratWidth/2 - slitWidth/2) ,filmThick,'base','corner','pos',{gratWidth/2 +
slitWidth/2,incidentThick + matchedThick},'rot','0');

g10=rect2(gratWidth, analyteThick,'base','corner','pos',{'0',incidentThick + matchedThick +
filmThick},'rot','0');

%create pmls
g11 = rect2(gratWidth, pmlThick, 'base', 'corner', 'pos', {0, -pmlThick}, 'rot', '0');
```

```
g12 = rect2(gratWidth, pmlThick, 'base', 'corner', 'pos', {0, incidentThick + matchedThick + filmThick +
analyteThick}, 'rot', '0');


% Analyzed geometry
clear s
s.objs={g2,g4,g6,g8,g10, g9, g11, g12};
s.name={'R1','R2','R3','R4','R5', 'R6', 'R7', 'R8'};
s.tags={'g2','g4','g6','g8','g10', 'g9', 'g11', 'g12'};

fem.draw=struct('s',s);
fem.geom=geomcsg(fem);

% Initialize mesh
fem.mesh=meshinit(fem, ...
   'hauto',5);

% Refine mesh
fem.mesh=meshrefine(fem, ...
   'mcase',0, ...
   'rmethod','regular');

% Refine mesh
fem.mesh=meshrefine(fem, ...
   'mcase',0, ...
   'rmethod','regular');



%create the progress bar
wait = waitbar(0, 'Progress...');

%start the number of cycles completed at 0
cycles = 0;

%set the nsp (returned surface plasmon index values) to an empty matrix
nsp = [];

%start the first n_eff at the original guess
n_eff = n_eff_guess;

for wavelength = wavelengthStart:waveIncrement:maxWavelength

   %reset n_eff_search flag
   n_eff_search = 1;

   %reset the total number of cycles used for the mode at this particular
   %wavelength
```

```
modeCycles = 0;

%reset the searchNum value which determines how many searches have been
%performed both above and below the current n_eff value being tested
searchNum = 1;

%search for the current n_eff as long as n_eff_search flag is true
while n_eff_search


    kf = 2*pi*n_eff/wavelength;


%%%%%%%%%%%%%%%%%%%%%%%%%%%%%%%%%%%%%%%%%%%%%%%%%%%%%%%%%%%%%%%%%%%%%%%%
%
    %%Solver data for determing the modes

%%%%%%%%%%%%%%%%%%%%%%%%%%%%%%%%%%%%%%%%%%%%%%%%%%%%%%%%%%%%%%%%%%%%%%%%
%


    % Application mode 1
    clear appl
    appl.mode.class = 'InPlaneWaves';
    appl.name = 'rfwh';
    appl.module = 'RF';
    appl.sshape = 2;
    appl.assignsuffix = '_rfwh';
    clear prop
    prop.analysis='eigen';
    prop.field='TM';
    appl.prop = prop;


    clear bnd
    bnd.type = {'SC','cont','periodic', 'SC'};


    bnd.kper = {{0;0},{0;0},{kf; gratWidth}, {0,0}};
    bnd.pertype = {'sym','sym','floque', 'sym'};
    bnd.ind = [3,4,3,2,3,2,3,2,3,2,3,2,1,2,2,2,2,2,2,3,3,3,3,3,3];
    appl.bnd = bnd;

    %    Set up the correct material properties for each subdomain...including
    %    PML's
    clear equ
    equ.coordOn = {{0;1},{0;0},{0;0},{0;0},{0,0}, {0;1}, {0;0}};
    equ.Stype = {'coord','none','none','none','none','coord','none'};
```

```
equ.n = {sqrt(eps_interp(incidentMat,wavelength)) ,... %1
    sqrt(eps_interp(incidentMat,wavelength)), ...       %2
    sqrt(eps_interp(matchedMat, wavelength)),...        %3
    sqrt(eps_interp(filmMat, wavelength)), ...          %4
    sqrt(eps_interp(analyteMat, wavelength)), ...       %5
    sqrt(eps_interp(analyteMat, wavelength)), ...       %6
    sqrt(eps_interp(slitMat, wavelength))};             %7

equ.matparams = 'n';
equ.ind = [1,2,3,4,5,6,7,4];
appl.equ = equ;



fem.appl{1} = appl;
fem.frame = {'ref'};
fem.border = 1;

clear units;
units.basesystem = 'SI';
fem.units = units;

% ODE Settings
clear ode
clear units;
units.basesystem = 'SI';
ode.units = units;
fem.ode=ode;

% Multiphysics
fem=multiphysics(fem);

% Extend mesh
fem.xmesh=meshextend(fem);

% Solve problem
% Note: eigref is necessary as it is a linearization point for the
% PMLs....without this a singularity occurs which will cause a fatal
% error.
fem.sol=femeig(fem, ...
    'conjugate','on', ...
    'solcomp',{'Hz'}, ...
    'outcomp',{'Hz'}, ...
    'blocksize','auto', ...
    'neigs', eigSolutions, ...
    'maxeigit', eigIter, ...
    'shift',-2*pi*3e8/(wavelength + 1e-15)*i, ...
    'eigref', num2str(-2*pi*3e8/(wavelength)*i));
```

```
% Save current fem structure for restart purposes
fem0=fem;


%loop through eigenvalues found to see if any match the set wavelength
for a = 1:eigSolutions
  eigWavelength = 3e8*2*pi/(abs(imag(fem.sol.lambda(a))));

   %get x and y locations outside of the film
  [x y] = meshgrid(0:1e-9:gratWidth, [0:5e-9:(incidentThick+matchedThick - 30e-9) (incidentThick +
matchedThick + filmThick + 30e-9):5e-9:(incidentThick+matchedThick+filmThick+analyteThick)]);

  outsideField = postinterp(fem, 'abs(Hz)', [x(:)';y(:)'], 'solnum', a);
  outsideMax = max(max(outsideField));


  %get x and y locations inside of the film
  [x y] = meshgrid(0:1e-9:gratWidth, (incidentThick + matchedThick - 30e-9):5e-9:(incidentThick +
matchedThick + filmThick + 30e-9));
  insideField = postinterp(fem, 'abs(Hz)', [x(:)';y(:)'], 'solnum', a);
  insideMax = max(max(insideField));

  %check for field enhancement and wavelength tolerance for
  %solution to be acceptable

  if(((abs(eigWavelength - wavelength ) < tolerance))&&(insideMax > outsideMax))
    %solution found...store the n_eff and plot the value
    figure(1);
    plot(wavelength*1e9, n_eff, 'o');
    hold on;

    %now plot the 2d field profile of the solution
    figure(2);
    postplot(fem, ...
      'tridata',{'Hz','cont','internal','unit','A/m'}, ...
      'trimap','Rainbow', ...
      'solnum',a, ...
      'title',['nu_rfwh(', num2str(a), ')', '=', num2str(eigWavelength*1e9), 'nm   Surface: Magnetic
field, z component [A/m]'], ...
      'axis',[-1E-7,gratWidth + 1e-7,-1e-7 - pmlThick,incidentThick + matchedThick + filmThick +
analyteThick + pmlThick + 1e-7]);

    %set the flag so that it stops searching and increments the
    %wavelength being tested
    n_eff_search = 0;

    %store the plasmon n_eff value into the nsp structure
```

```
            nsp = [nsp, n_eff];

            %change n_eff for the next guess according to the current
            %slope based on this found n_eff and the previous one to
            %speed up the calculations.
            n_eff_temp = n_eff;

            n_eff = 2*n_eff - n_eff_previous;

            n_eff_previous = n_eff_temp;

%               %Determine the S value in the teflon to check whether or
%               %not it is bound;
%               nu = abs(imag(fem.sol.lambda(a)))/(2*pi);
%               Beta = 2*pi/wavelength*(n_eff - i*real(fem.sol.lambda(a)));
%               S3 = sqrt(Beta^2 - eps_interp('teflonaf_cauchy', wavelength)*(2*pi/wavelength)^2);
%               figure(3);
%               plot(wavelength*1e9, real(S3), 'ro');
%               hold on;


            break;

         end
      end

      %You are still searching after finding the eigenvalues, the n_eff
      %value needs to be increased/decreased even further from the
      %original guess.  Every other cycle search a higher value, and
      %every other cycle search an even lower value from the original
      %guess.  This allows the search to follow both increasing and
      %decreasing dispersion curves.
      if(n_eff_search)
         if(~mod(modeCycles,2))
            n_eff = n_eff + n_eff_step*searchNum;
            searchNum = searchNum + 1;
         else
            n_eff = n_eff - n_eff_step*searchNum;
            searchNum = searchNum + 1;
         end
      end

      %increment the number of cycles performed at this particular
      %wavelength
      modeCycles = modeCycles + 1;

   end
```

```
    %increment the number of total cycles performed for the outer for loop
    %(number of n_eff's found total, and update the progress bar once an
    %n_eff has been found.
    cycles = cycles + 1;
    waitbar(cycles/length(wavelengthStart:waveIncrement:maxWavelength), wait);

end

%populate the wavelength vector searched
wavelength = wavelengthStart:waveIncrement:maxWavelength;

%nsp = fliplr(nsp);

%save the resulting dispersion data to a file
save './Importon Curves/sr_burke_pt2_062809' wavelength nsp;

%close the progress bar
close(wait);
```

Appendix C: RCWT Reflectivity Code

```
%%%%%%%%%%%%%%%%%%%%%%%%%%%%%%%%%%%%%%%%%%%%%%%%%%%%%%%%%
%%%%%%%%%%%%%%%%%%%%%%
%calcSPRLambdaSlits.m
%
%Script using RCWT calculator from OptiScan (Arizona State) to plot the SPR output
%reflectivity at a single wavelength when plane wave (TM for plasmon coupling) is incident onto
%a metal film (e.g. gold) with nano-gaps placed within the metal film.
%Note that in this script there is no input for slit material, thus the
%slit is always taken as having the index of the analyte solution (a
%complete slit in the material).  This could be modified in the future,
%thus the variable n_slit is left for change.
%
% notes:
% lambda is specified in nm.
% slitlayer, toplayer and background are binary terms specifying whether a background/bound layer should
be modeled
%
% function R = calcSPRLambdaSlits(incident, matchedMaterial, substrate, rodMaterial, lambda, theta,
gratWidth, slitWidth, ...
%     filmThick, matchedThick, m, polarization, slitlayer, toplayer, background)
%
%Description of inputs:
%   incident - incident material data file (usually the prism material)
%   matchedMaterial - material data file of the matched layer (usually Teflon)
%   substrate - material data file of the analyte solution (substrate in
%       this case as RCWT flips the incident order)
%   rodMaterial - material data file of the plasmon supporting film
%   lambda - wavelength to test in nm
%   theta - angle of incident light in degrees
%   gratWidth - width of one period of the structure (which is inherently a
%       grating
%   filmThick - thickness of the plasmon supporting film
%   matchedThick - thickness of the matched material
%   slitWidth - width of the slit
%   m - number of diffracted orders to solve for (must be high enough to
%       converge to accurate solutionn, however if too high the matrices
%       will become such that they are singular and the calculation may be
%       innacurrate).
%   polarization - 'TE' or 'TM'
%   slitlayer - binding at matched surface in slit
%   toplayer - binding at plasmon supporting material surface
%   background - background index shift
%
%Description of output:
%   R – reflectivity
%
%Code written by Phillip D. Keathley
%Last Updated: 08/06/09

function R = calcSPRLambdaSlits(incident, matchedMaterial, substrate, rodMaterial, lambda, theta,
gratWidth, slitWidth, ...
    filmThick, matchedThick, m, polarization, slitlayer, toplayer, background)
```

```
%set the wavelengths used for the green/red regions
lambda = lambda*1e-9;


%get index values in each region; These will stay the same as they are
%physical properties of the materials.  It is necessary to interpolate the
%index values at the specified lambda values for the desired spectral
%region.
n_incident = index_interp(incident, lambda);%ones(1,length(n_metal));%index_interp(incident, lambda) +
.000982*32.3; %compensate for 32.2% ethylene glycol mixture in water

n_sub = index_interp(substrate, lambda) + j*1e-15; %index_interp(substrate, lambda);

%if background shift then shift n_sub
if(background)
   n_sub = n_sub + .0005;
end

n_rod = index_interp(rodMaterial, lambda);

n_matched = index_interp(matchedMaterial, lambda);

%for this script, the slit material is always the same as the substrate
%(analyte solution) material as there is no input for slit material in the
%function.  This could be updated for newer sensor designs.
n_slit = n_sub;

%set initial values of phi and psi
phi = 0; %angle that the incoming light makes around the x-axis



%set up the rod characteristics to be in the grating.
%remember that dimensions are in nm
rodWidth = gratWidth - slitWidth;
rodHeight = filmThick;

%now create the grating profile with the above entered information

%column vector of layer heights
Grating.h = 1e-9*[matchedThick; 1; rodHeight - 1; 1];

%Create empty data matrices for the index profile, as these will be filled
%in one at a time for each wavelength in the following Diff-Eff
%calculations to accomodate for dispersion.
Grating.ng1 = [];
Grating.ng2 = [];
Grating.n1 = [];
Grating.n2 = [];

%Create the grating profile for each layer.  Each row tells at what
%percentage of the length of the grating pitch to switch to the second
%index value specified for that layer.
%Layers:
% 1) Teflon/index matched layer
```

```
% 2) gold with slit & bound material on teflon/matched material surface
% 3) gold with slit (no bound layer)
% 4) bound material over top of gold beside the slits
Grating.cperd = [1,1,1;...
   (gratWidth - rodWidth)/(2*gratWidth), (gratWidth + rodWidth)/(2*gratWidth), 1; ...
   (gratWidth - rodWidth)/(2*gratWidth), (gratWidth + rodWidth)/(2*gratWidth), 1; ...
   (gratWidth - rodWidth)/(2*gratWidth), (gratWidth + rodWidth)/(2*gratWidth), 1];

%the grating period in meters
Grating.d = gratWidth*1e-9;




%set to correct polarization
if(strcmp(polarization, 'TM'))
   psi = 0;
elseif(strcmp(polarization, 'TE'))
   psi = 90;
end



%set up the grating material profile

%ng1 and ng2 are column vectors that give the first and second index
%values respectively for each layer

%first index values for layers 1 and 2
Grating.ng1(1,1) = n_matched;

%check to see if the bound layers should be added....if so, add them!
if(slitlayer)
   Grating.ng1(2,1) = 1.45;
else
   Grating.ng1(2,1) = n_slit;
end


Grating.ng1(3,1) = n_slit;

Grating.ng1(4,1) = n_sub;


%second index values for layers 1 and 2
Grating.ng2(1,1) = n_matched;
Grating.ng2(2,1) = n_rod;
Grating.ng2(3,1) = n_rod;

if(toplayer)
   Grating.ng2(4,1) = 1.45;
else
   Grating.ng2(4,1) = n_sub;
end
```

```
%indices of incident and substrate materials
%note that only the real part of the incident index is taken
%as an imaginary part will lead unphysical results (the incident
%material is assumed semi-infinite, thus the light would never make it
%to the sample if enven the smallest absorption is present)
Grating.n1 = real(n_incident);
Grating.n2 = n_sub;

[Rspr Tspr] = output_generator(Grating,m,phi,psi,theta,lambda);

%Return the reflectivity value only for SPR calculations
R = Rspr;
```

```
%%%%%%%%%%%%%%%%%%%%%%%%%%%%%%%%%%%%%%%%%%%%%%%%%%%%%%%%%%%%%%%%%%%%%%%%%%%%%%%%
%calcSPRspectrumSlits.m
%
%Script using RCWT from OptiScan (Arizona State) to plot the SPR output
%spectrum when plane wave (TM for plasmon excitation) is incident onto a
%grating consisting of slits (nano-gaps) in a gold film.
%
%Description of inputs:
%   incident - incident material data file (usually the prism material)
%   matchedMaterial - material data file of the matched layer (usually Teflon)
%   substrate - material data file of the analyte solution (substrate in
%       this case as RCWT flips the incident order)
%   rodMaterial - material data file of the plasmon supporting film
%   slitMaterial - material data file of the slit
%   incr - wavelength increment in nm
%   start - start wavlength in nm
%   stop - stop wavelength in nm
%   theta - angle of incident light in degrees
%   gratWidth - width of one period of the structure (which is inherently a
%       grating
%   filmThick - thickness of the plasmon supporting film
%   matchedThick - thickness of the matched material
%   slitWidth - width of the slit
%   m - number of diffracted orders to solve for (must be high enough to
%       converge to accurate solutionn, however if too high the matrices
%       will become such that they are singular and the calculation may be
%       innacurrate).
%
%Description of outputs:
%   Rtm - TM reflectivity
%   Rte - TE reflectivity
%
%Coded written by Phillip D. Keathley
%Last Updated: 8/6/09


function [Rtm Rte] = calcSPRspectrumSlits(incident, matchedMaterial, substrate, rodMaterial, slitMaterial,
incr, start, stop, theta, gratWidth, slitWidth, ...
   filmThick, matchedThick, m)


%set the wavelengths used for the green/red regions
lambda = start:incr:stop;
lambda = lambda*1e-9;



%get index values in each region; These will stay the same as they are
%physical properties of the materials.  It is necessary to interpolate the
%index values at the specified lambda values for the desired spectral
%region.
n_incident = index_interp(incident, lambda);%ones(1,length(n_metal));%index_interp(incident, lambda) +
.000982*32.3; %compensate for 32.2% ethylene glycol mixture in water

n_sub = index_interp(substrate, lambda) + j*1e-15; %index_interp(substrate, lambda);
```

```
n_rod = index_interp(rodMaterial, lambda);

n_matched = index_interp(matchedMaterial, lambda);

n_slit = index_interp(slitMaterial, lambda);

%set initial values of phi and psi
phi = 0; %angle that the incoming light makes around the x-axis
psi = 0; %angle of polarization (0 degrees is TM or S polarized, 90 TE or P polarized)


%set up the rod characteristics to be in the grating.
%remember that dimensions are in nm
rodWidth = gratWidth - slitWidth;
rodHeight = filmThick;

%now create the grating profile with the above entered information

%column vector of layer heights
Grating.h = 1e-9*[matchedThick; rodHeight];

%Create empty data matrices for the index profile, as these will be filled
%in one at a time for each wavelength in the following Diff-Eff
%calculations to accomodate for dispersion.
Grating.ng1 = [];
Grating.ng2 = [];
Grating.n1 = [];
Grating.n2 = [];

%Create the grating profile for each layer.  Each row tells at what
%percentage of the length of the grating pitch to switch to the second
%index value specified for that layer.
Grating.cperd = [1,1,1;(gratWidth - rodWidth)/(2*gratWidth), (gratWidth + rodWidth)/(2*gratWidth), 1];

%the grating period in meters
Grating.d = gratWidth*1e-9;

wait = waitbar(0, 'Progress...');

for a=1:length(lambda)

    %set to TM for SPR coupling
    psi = 0;

    %set up the grating material profile

    %ng1 and ng2 are column vectors that give the first and second index
    %values respectively for each layer

    %first index values for layers 1 and 2
    Grating.ng1(1,1) = n_matched(a);
    Grating.ng1(2,1) = n_slit(a);

    %second index values for layers 1 and 2
    Grating.ng2(1,1) = n_matched(a);
    Grating.ng2(2,1) = n_rod(a);
```

```
    %indices of incident and substrate materials
    %note that only the real part of the incident index is taken
    %as an imaginary part will lead unphysical results (the incident
    %material is assumed semi-infinite, thus the light would never make it
    %to the sample if enven the smallest absorption is present)
    Grating.n1 = real(n_incident(a));
    Grating.n2 = n_sub(a);

    [Rspr(a) Tspr(a)] = output_generator(Grating,m,phi,psi,theta,lambda(a));

    %take TE polarization as reference
    psi = 90;

    %now calculate the reference spectrum
    [RsprR(a) TsprR(a)] = output_generator(Grating,m,phi,psi,theta,lambda(a));

    waitbar(a/length(lambda), wait);

end

%close the progress bar
close(wait);

%Return values of the reflectivity, and the reference reflectivity with
%TE polarization
Rtm = Rspr;
Rte = RsprR;
```

```
%%%%%%%%%%%%%%%%%%%%%%%%%%%%%%%%%%%%%%%%%%%%%%%%%%%%%%%%%%%%%%%%%%%%%%
%%%%%%%%%%%%%%%%%%%%%%
%output_generator.m
%
%Function to generate the reflectivity data from incident light of the
%given lambda, thetain, phiin and psiin using RCWT calculations from
%OptiScan (Univ. of Arizona).
%
%Description of inputs:
%   Grating - grating structure consistent with style defined in Optiscan
%   m - number of diffracted orders to calculate in the RCWT calculations
%   phiin - angle about x of incident light in degrees (usually 0)
%   psiin - angle of polarization of incident light in degrees
%   lambda - wavelength (in vacuum) of incident light
%
%Description of outputs
%   Rspr - reflectivity (zeroth order only)
%   Tspr - transmission (zeroth order only)
%
%This function written by Phillip D. Keathley.  DiffEffRCWT was unmodified
%and is taken directly from the Optiscan package.
%
%last updated 8/6/09

function [Rspr Tspr] = output_generator(Grating,m,phiin,psiin,thetain,lambda)


[DErs,DErp,DEts,DEtp]=DiffEffRCWT(Grating,m,phiin,psiin,thetain,lambda);

%zeroth order in middle of array (m+1)
Rspr=DErp(m+1)+DErs(m+1);
Tspr = DEtp(m+1)+DEts(m+1);
```

Appendix D: LOD Calculation Code

```
%%%%%%%%%%%%%%%%%%%%%%%%%%%%%%%%%%%%%%%%%%%%%%%%%%%%
%%%%%%%%%%%%%%%%%%%
%twoValueLOD_minimumSearch_slits.m
%
%Script to find the minimum LOD for a multi-moded sensor with a periodic array of
%nano-gaps.  It determines the sensor LOD when determining the binding
%thickness of one material bound to the gold and on the teflon in the gap.
%It also returns the LOD of the sensor for the calculation of background index change.
%
%Code written by Phillip D. Keathley
%Last updated: 8/6/09

clear all;

%set up the lambda values to search through to determine LOD
%this will be used in the loops that essentially integrate the reflectivity
%function for LOD determination.  Essentially they are limited by the
%spectrometer to be used which only has a range of 400 to 1000 nanometers.
lambdaStart = 400;
lambdaEnd = 1000;
lambdaStep = 2;

%get photon density...usually just 1 for theoretical modeling.  However it
%should be noted that this value changes with wavelength for a typical
%source and detector, thus shifting the sensor design to achieve minimal
%LOD...
P = 1;

%For convenience, make the lambda shift (deltaLambda) half of the lambda
%step.  For small enough of a lambdaStep, changing this value should not
%greatly alter the results.
deltaLambda = lambdaStep/2;

%populate the lambdas to be integrated from the above information assuming
%that deltaLambda = 1/2*lambdaStep.
lambdas = (lambdaStart - deltaLambda:lambdaStep:lambdaEnd + deltaLambda);

%Set a threshold for the minimum search.  Minima above this threshold will
%be ignored.  Those below will be tracked.  For the two-value problem,
%there must be at least two minima, but no limit on the amount over two.
modeThreshold = .75;

%Set the material data file names to be passed to reflectivity function.
incident = 'bk7_vase';
matchedMaterial = 'teflonaf_cauchy';
substrate = 'water_crc';
rodMaterial = 'gold_jc';
slitMaterial = 'water_crc';

%Set wavelength data moved to the right by deltaX/2 (this will be
%the shift for determining the minimum variance for each mode).
incr = lambdaStep;
start = lambdaStart - deltaLambda;
```

```
stop = lambdaEnd + deltaLambda;

%Set the theta(s) to be searched through for LOD minimization.
theta = 62.5;

%Set dimensions of slit periodicity (grating width) and slit width.  Make
%them vectors if you wish to sift through them for the LOD search.
gratWidth = 160;
slitWidth = 20;

%Set the thickness of the films... make these two values vectors if you
%wish to sift through them for an LOD minimization search.
filmThick = 39:3:60;
matchedThick = 350:25:800;

%Set number of diffracted orders to calculate for RCWT process.  Typically
%20 is sufficient for accurate results.
m = 20;


%Now calculate spectral density data for use with LOD calculations to
%provide a physically accurate LOD determination based on the spectrometer
%and source used.

% note - this spectrum has the dark level subtracted
import_spectrum = importdata('sub dark - 1ms - 0avg - 0box.Master.Sample');
spectrum = import_spectrum.data;

%note dl_spect is not a constant across the spectrum, therefore for proper
%interpolation one must take the spectral density (spect_den).
dl_spect = diff(spectrum(:,1));
spect_den = spectrum(1:3647,2)./dl_spect;

%calculate the normalized spectral density
spect_den_normal = spect_den/(max(spect_den));

%interpolate the data for the sampling grid used for LOD calculation
spect_den_norm_interp = interp1(spectrum(1:3647,1),spect_den_normal,lambdas,'spline');

%%%%%%%%%%%%%%%%%%%%%%%%%%%%%%%%%%%%%%%%%%%%%%%%%%
%%%%%%%%%
%From this point the LOD calculation must be looped through for iterating
%the following variables:
%
% (a) theta
% (b) gratWidth
% (c) slitWidth
% (d) filmThick
% (e) matchedThick
%
%This will create a 5 dimension matrix holding the LOD for each dimension.
%For each point in the matrix LOD(a,b,c,d,e) will be the value of the LOD
%for each variable value of a,b,c,d,e respectively. This amounts to
%a*b*c*d*e iterations.

%Create a waitbar for overall progress.
```

```
overallProgress = waitbar(0, 'Overall Progress...');
totalLength =
length(theta)*length(gratWidth)*length(slitWidth)*length(filmThick)*length(matchedThick);

%set variable loops to keep track of total number of cycles completed.
loops = 0;

for a=1:length(theta)
   for b = 1:length(gratWidth)
      for c = 1:length(slitWidth)
         for d = 1:length(filmThick)
            for e = 1:length(matchedThick)

               %Clear variables to be overwritten one component at a
               %time as their lengths will change.
               clear minVar;
               clear Slayer;
               clear Sbackground;



               %Call the function to get the reflectivity data for TM and TE with the
               %desired settings for the entire spectrum.
               [Rtm Rte] = calcSPRspectrumSlits(incident, matchedMaterial, substrate, rodMaterial,
slitMaterial, incr, start, stop, theta(a), gratWidth(b), slitWidth(c), ...
                  filmThick(d), matchedThick(e), m);

               %Now for the determination of the minimum variance for the determination of
               %dletaLambda for each mode present.  First the modes must be found and
               %inflection points determined.
               [bounds boundValues mins minValues] = findIntegrationBounds(Rtm, modeThreshold);

               %check to see that there are at least two
               %minimums...else don't waste your time, there won't be
               %a solution!
               if(length(mins) >= 2)


                  %find the minimum variance for each mode found.

                  dR_dLambda = diff(Rtm)/lambdaStep;

                  wait = waitbar(0, 'Calculating Variances');

                  for minNum = 1:length(mins)

                     %calculate the minimum variance using the Cramer Rao bound (from Howard and
                     %Pien's paper).
                     minVar(minNum) =
(P*lambdaStep*sum((dR_dLambda(bounds(minNum):bounds(minNum+1)).^2).*spect_den_norm_interp(
bounds(minNum):bounds(minNum+1))./Rtm(bounds(minNum):bounds(minNum+1))))^-1;

                     waitbar(minNum/length(mins), wait);
                  end
```

```
waitbar(0, wait, 'Calculating Sensitivities and Solving');

%Sensitivity determination for each mode using fminbnd
options = optimset('TolX',1e-12);
for minNum = 1:length(mins)

   %determine the appropriate bounds for the
   %minimum search
   if((lambdas(mins(minNum)) - 30) < lambdas(bounds(minNum)))
      leftMinSearchBound = lambdas(bounds(minNum));
   else
      leftMinSearchBound = lambdas(mins(minNum)) - 30;
   end

   if((lambdas(mins(minNum)) + 30) > lambdas(bounds(minNum+1)))
      rightMinSearchBound = lambdas(bounds(minNum + 1));
   else
      rightMinSearchBound = lambdas(mins(minNum)) + 30;
   end


   %determine the minima and their locations for the original spectrum
   [mode_lambda, mode_min] = fminbnd(@(wavelength) calcSPRLambdaSlits(incident,
matchedMaterial, substrate, rodMaterial, wavelength, theta(a), gratWidth(b), slitWidth(c), ...
      filmThick(d), matchedThick(e), m, 'TM', 0, 0, 0),leftMinSearchBound,
rightMinSearchBound, options);

   %determine minima and their locations for the spectrum with a top bound
   %layer
   [mode_lambda_layer, mode_min_layer] = fminbnd(@(wavelength)
calcSPRLambdaSlits(incident, matchedMaterial, substrate, rodMaterial, wavelength, theta(a), gratWidth(b),
slitWidth(c), ...
      filmThick(d), matchedThick(e), m, 'TM', 1, 1, 0), leftMinSearchBound,
rightMinSearchBound, options);

   %determine minima and their locations for the spectrum with a
   %background index change
   [mode_lambda_background, mode_min_background] = fminbnd(@(wavelength)
calcSPRLambdaSlits(incident, matchedMaterial, substrate, rodMaterial, wavelength, theta(a), gratWidth(b),
slitWidth(c), ...
      filmThick(d), matchedThick(e), m, 'TM', 0, 0, 1), leftMinSearchBound,
rightMinSearchBound, options);

   %calculate sensitivities based on 1 nm thickness bound layers and .001
   %index background shift.
   Slayer(minNum) = (mode_lambda_layer - mode_lambda);
   Sbackground(minNum) = (mode_lambda_background - mode_lambda)/.0005;

   waitbar(minNum/length(mins), wait);
end

close(wait);

%calculate A matrix for Ax = B, where x is the column vector of parameters
%to be detected and B is the column vector of shifts in wavelength for each
%mode...note that this will be an overdetermined system if there are 4
```

```
                %modes (which there should be).
                A = [Slayer', Sbackground'];

                %now using A, find solutionMatrix = (A'*A)^-1*A'.  Thus x =
                %solutionMatrix*B;  var(x) = variance(solutionMatrix*B) =
                %solutionMatrix.^2*var(B)...where var(B) = minVar'

                solutionMatrix = (A'*A)^-1*A';

                varX = solutionMatrix.^2*minVar';

                varLayer = varX(1,1);
                varBackground = varX(2,1);

                %print out the found LOD's
                layerLOD(a,b,c,d,e) = 3*sqrt(varLayer);
                backgroundLOD(a,b,c,d,e) = 3*sqrt(varBackground);

                figure(1);
                plot(lambdas, Rtm, 'k', lambdas(bounds), Rtm(bounds), 'ro', lambdas(mins), Rtm(mins),
'bo');
                legend('Reflectivity', 'Integration Bounds', 'Minimums Tracked');
                title({['Reflectivity Vs. Wavelength'];['Layer LOD: ' num2str(layerLOD(a,b,c,d,e)) ',
Background LOD: ' num2str(backgroundLOD(a,b,c,d,e))]});
                hold off;

            else
                %not enough minimums to compute a solution...LOD
                %must be NaN
                layerLOD(a,b,c,d,e) = NaN;
                backgroundLOD(a,b,c,d,e) = NaN;
            end

            loops = loops + 1;
            %update the overall progress waitbar.
            waitbar(loops/totalLength, overallProgress);

        end
      end
    end
  end
end

%close the overallProgress bar
close(overallProgress);

%save the data to a file for later analysis
save ../../../lodResults/071509/minimumExpanded_1 backgroundLOD layerLOD filmThick matchedThick
theta gratWidth slitWidth
```

```
%%%%%%%%%%%%%%%%%%%%%%%%%%%%%%%%%%%%%%%%%%%%%%%%%%%%%%%%
%%%%%%%%%%%%%%%%%%%%%%%%
%findIntegrationBounds.m
%
%Function used to determine the integration bounds in order to determine
%the LOD of plasmon modes given an input spectrum and minimum threshold
%value.  The value of the first bound and last bound both include the
%beginning and end of the spectrum to be analyzed.  If no mins are found,
%then the mins are returned as NaN.
%
%Description of inputs:
%   R - reflectivity data (vector)
%   threshold - threshold value for determining a minimum
%
%Description of outputs:
%   bounds - bound index values for each minimum found
%   boundValues - reflectivity value at the bound location
%   mins - indices for minima found
%   minValues - reflectivity values for all minima
%
% Written by Donnie Keathley
% Last Updated: 8/6/09


function [bounds boundValues mins minValues] = findIntegrationBounds(R, threshold)

difference = diff(R);

bounds(1) = 1; %default value is the left of the window
boundValues(1) = R(1);

%default value for mins/minValues is NaN.  This will be overwritten if a
%minimum is found.
mins = NaN;
minValues = NaN;

bndIndex = 2;
minIndex = 1;

slope = -1;

%flag to determine if a minimum has been found
minFlag = 0;

for a = 2:length(difference)

   if(slope < 0)

      %the direction is downward.  If this changes you have found a min
      if(difference(a) > 0)

         %a min has been found, set new slope and check the threshold
         slope = 1;

         if((R(a) <= threshold) && (minFlag == 0))
```

```
            %set the appropriate minimum index and value
            mins(minIndex) = a;
            minValues(minIndex) = R(a);

            minIndex = minIndex + 1;

            %set minFlag
            minFlag = 1;

         elseif(R(a) <= threshold && (R(a) < minValues(minIndex - 1)))
            %this minimum is less than the previous, but a bound hasn't
            %been set so set this to the minimum
            mins(minIndex - 1) = a;
            minValues(minIndex - 1) = R(a);

         end

      end

      %if slope hasn't changed, then do nothing

   else

      %this means the direction is upward.  If this changes you have a
      %maximum...however you only care if the minFlag is on, and the maximum is above the threshold as
this
      %implies the maximum becomes an inflection point.

      if(difference(a) < 0)

         %a max has been found, set the new slope
         slope = -1;

         if(minFlag && (R(a) > (minValues(minIndex - 1) + .05)) )

            %if minFlag is positive, this is an inflection point.  Set
            %it as such and invert minFlag.

            bounds(bndIndex) = a;
            boundValues(bndIndex) = R(a);

            bndIndex = bndIndex + 1;

            minFlag = 0;

         end
      end
   end

end
```

```
%by default the last bound is the end of the window, set it as such only if
%the minFlag is set (there is a minimum in front of it)
if(minFlag)
   bounds(bndIndex) = length(difference);
   boundValues(bndIndex) = R(end-1);
end
```

Appendix E: Cross Section Determination Code

```
%%%%%%%%%%%%%%%%%%%%%%%%%%%%%%%%%%%%%%%%%%%%%%%%%%%%%
%%%%%%%%%%%%%%%%%%%%%%
%fieldProfileanalysis.m
%
%Code for determining field profiles at various locations within the
%defined structure (nano-gaps periodically cut into a plasmon supporting
%film).  This allows one to study the fields of plasmon modes that are
%excited at the specified wavelength and angle for the defined structure.
%Comsol used to calculate and interpolate the fields (see
%slitsModeSearch.m).
%
%Code written by Phillip D. Keathley
%last modified 8/6/09

%Define the structure parameters
incidentThick = 10000e-9;
matchedThick = 575e-9;
filmThick = 39e-9;
slitWidth = 20e-9;
gratWidth = 160e-9;
analyteThick = 5000e-9;
pmlThick = 1000e-9;

%distances above and below the film to plot
distanceAboveFilm = 2000e-9;
distanceBelowFilm = 600e-9;

lambda = 875e-9;
theta = 62.5;

% function femPlot = slitsModeSearch(incidentMat, matchedMat, filmMat, analyteMat, ...
%     slitMat, wavelength, theta, ...
%     gratWidth, filmThick, analyteThick, matchedThick, incidentThick, slitWidth, pmlThick, ...
%     maxIter);


%Calculation the fields inside the structure using slitsModeSearch
fem = slitsModeSearch('bk7_vase', 'teflonaf_cauchy', 'gold_jc', 'water_crc', ...
    'water_crc', lambda, theta, ...
    gratWidth, filmThick, analyteThick, matchedThick, incidentThick, slitWidth, pmlThick, ...
    300); %last value is number of iterations to perform for harmonic analysis.

figure();

%get line to determine field profile at given x location
x = 0e-9;
filmCenter = incidentThick + matchedThick + filmThick/2;

%y inside of the film
y = (incidentThick + matchedThick - distanceBelowFilm):1e-9:(incidentThick + matchedThick);

fieldProfileCenter_below = postinterp(fem, 'abs(Hz)', [x*ones(1,length(y));y]);
```

```
subplot(1,2,1);
plot((y - filmCenter)*1e9, fieldProfileCenter_below, 'r');
hold on;

%y inside of the film
y = (incidentThick + matchedThick):1e-9:(incidentThick + matchedThick + filmThick);

fieldProfileCenter_film = postinterp(fem, 'abs(Hz)', [x*ones(1,length(y));y]);

subplot(1,2,1);
plot((y - filmCenter)*1e9, fieldProfileCenter_film, 'g');

%y inside of the film
y = (incidentThick + matchedThick + filmThick):1e-9:(incidentThick + matchedThick + filmThick +
distanceAboveFilm);

fieldProfileCenter_above = postinterp(fem, 'abs(Hz)', [x*ones(1,length(y));y]);

subplot(1,2,1);
plot((y - filmCenter)*1e9, fieldProfileCenter_above, 'b');


xlabel('Distance Above Center of Film (nm)');
ylabel('abs(H) Relative');
title('Magnetic Field Strength Relative To Incident Magnitude In Film');
legend('Below Film', 'In Film', 'Above Film');



%get line to determine field profile at given x location
x = gratWidth/2;
filmCenter = incidentThick + matchedThick + filmThick/2;

%y inside of the film
y = (incidentThick + matchedThick - distanceBelowFilm):1e-9:(incidentThick + matchedThick);

fieldProfileCenter_below = postinterp(fem, 'abs(Hz)', [x*ones(1,length(y));y]);

subplot(1,2,2);
plot((y - filmCenter)*1e9, fieldProfileCenter_below, 'r');
hold on;

%y inside of the film
y = (incidentThick + matchedThick):1e-9:(incidentThick + matchedThick + filmThick);

fieldProfileCenter_film = postinterp(fem, 'abs(Hz)', [x*ones(1,length(y));y]);

subplot(1,2,2);
plot((y - filmCenter)*1e9, fieldProfileCenter_film, 'g');

%y inside of the film
y = (incidentThick + matchedThick + filmThick):1e-9:(incidentThick + matchedThick + filmThick +
distanceAboveFilm);

fieldProfileCenter_above = postinterp(fem, 'abs(Hz)', [x*ones(1,length(y));y]);
```

```
subplot(1,2,2);
plot((y - filmCenter)*1e9, fieldProfileCenter_above, 'b');

%label the plot
xlabel('Distance Above Center of Film (nm)');
ylabel('abs(H) Relative');
title('Magnetic Field Strength Relative To Incident Magnitude In Slit');
legend('Below Film', 'In Film', 'Above Film');


figure();

%now for a slice across the x direction at a y value;

%get line to determine field profile at given y location
filmCenter = incidentThick + matchedThick + filmThick/2;
y = filmCenter + filmThick/2;

%fist plot the region in the film
x = 0:1e-9:(gratWidth/2 - slitWidth/2);

fieldProfileCenter_leftFilm = postinterp(fem, 'abs(Hz)', [x;y*ones(1,length(x))]);

subplot(3,1,1);
plot(x*1e9, fieldProfileCenter_leftFilm, 'g');
hold on;

%fist plot the region in the film
x = (gratWidth/2 - slitWidth/2):1e-9:(gratWidth/2 + slitWidth/2);

fieldProfileCenter_slit = postinterp(fem, 'abs(Hz)', [x;y*ones(1,length(x))]);

subplot(3,1,1);
plot(x*1e9, fieldProfileCenter_slit, 'r');

%fist plot the region in the film
x = (gratWidth/2 + slitWidth/2):1e-9:gratWidth;

fieldProfileCenter_rightFilm = postinterp(fem, 'abs(Hz)', [x;y*ones(1,length(x))]);

subplot(3,1,1);
plot(x*1e9, fieldProfileCenter_rightFilm, 'g');


xlabel('Distance Along Film (nm)');
ylabel('abs(H) Relative');
title('Magnetic Field Strength Relative To Incident Magnitude In Slit (Film Top)');
legend('Left Film', 'Slit', 'Right Film');


%get line to determine field profile at given y location
y = filmCenter;

%fist plot the region in the film
x = 0:1e-9:(gratWidth/2 - slitWidth/2);
```

```
fieldProfileCenter_leftFilm = postinterp(fem, 'abs(Hz)', [x;y*ones(1,length(x))]);

subplot(3,1,2);
plot(x*1e9, fieldProfileCenter_leftFilm, 'g');
hold on;

%fist plot the region in the film
x = (gratWidth/2 - slitWidth/2):1e-9:(gratWidth/2 + slitWidth/2);

fieldProfileCenter_slit = postinterp(fem, 'abs(Hz)', [x;y*ones(1,length(x))]);

subplot(3,1,2);
plot(x*1e9, fieldProfileCenter_slit, 'r');

%fist plot the region in the film
x = (gratWidth/2 + slitWidth/2):1e-9:gratWidth;

fieldProfileCenter_rightFilm = postinterp(fem, 'abs(Hz)', [x;y*ones(1,length(x))]);

subplot(3,1,2);
plot(x*1e9, fieldProfileCenter_rightFilm, 'g');

xlabel('Distance Along Film (nm)');
ylabel('abs(H) Relative');
title('Magnetic Field Strength Relative To Incident Magnitude In Slit (Film Center) ');
legend('Left Film', 'Slit', 'Right Film');

%get line to determine field profile at given y location
y = filmCenter - filmThick/2;

%fist plot the region in the film
x = 0:1e-9:(gratWidth/2 - slitWidth/2);

fieldProfileCenter_leftFilm = postinterp(fem, 'abs(Hz)', [x;y*ones(1,length(x))]);

subplot(3,1,3);
plot(x*1e9, fieldProfileCenter_leftFilm, 'g');
hold on;

%fist plot the region in the film
x = (gratWidth/2 - slitWidth/2):1e-9:(gratWidth/2 + slitWidth/2);

fieldProfileCenter_slit = postinterp(fem, 'abs(Hz)', [x;y*ones(1,length(x))]);

subplot(3,1,3);
plot(x*1e9, fieldProfileCenter_slit, 'r');

%fist plot the region in the film
x = (gratWidth/2 + slitWidth/2):1e-9:gratWidth;

fieldProfileCenter_rightFilm = postinterp(fem, 'abs(Hz)', [x;y*ones(1,length(x))]);

subplot(3,1,3);
plot(x*1e9, fieldProfileCenter_rightFilm, 'g');

xlabel('Distance Along Film (nm)');
```

```
ylabel('abs(H) Relative');
title('Magnetic Field Strength Relative To Incident Magnitude In Slit (Film bottom)');
legend('Left Film', 'Slit', 'Right Film');
```

Appendix F: Material Dispersion Interpolation Code

```
%%%%%%%%%%%%%%%%%%%%%%%%%%%%%%%%%%%%%%%%%%%%%%%%%%%%%%%%
%%%%%%%%%%%%%%
%eps_interp.m
%
%Function to interpolate the dielectric constant dispersion of a given
%material given its material properties file specified by filename at the
%specified wavelength, lambda.
%
%Description of inputs:
%   filename - filename of material data file
%   lambda - wavelength to perform interpolation for
%
%Description of outputs:
%   eps - interpolated dielectric constant
%
%Code written by, and used with permission from, J. Todd Hastings

function eps = eps_interp(filename,lambda)

%lambda should be specified in meters
load(filename);
nint = interp1(wavelength,n,lambda,'spline');
kint = interp1(wavelength,-k,lambda,'spline');
eps = (nint+kint*j).^2;

%%%%%%%%%%%%%%%%%%%%%%%%%%%%%%%%%%%%%%%%%%%%%%%%%%%%%%%%
%%%%%%%%%%%%%%
%index_interp.m
%
%Function to interpolate the refractive index dispersion of a given
%material given its material properties file specified by filename at the
%specified wavelength, lambda.
%
%Description of inputs:
%   filename - filename of material data file
%   lambda - wavelength to perform interpolation for
%
%Description of outputs:
%   n - interpolated refractive index
%
%Code written by Phillip D. Keathley

function n = index_interp(filename,lambda)
%lambda should be specified in meters
load(filename);
nint = interp1(wavelength,n,lambda);
kint = interp1(wavelength,k,lambda);
n = nint + j*kint;
```

References

[1] J. J. Burke, G. I. Stegeman, and T. Tamir, "Surface-polariton-like waves guided by thin, lossy metal films," *Physical Review B,* vol. 33, p. 16, 15 April 1986.

[2] H. Raether, *Surface plasmons on smooth and rough surfaces and on gratings*. New York: Springer-Verlag, 1988.

[3] J. Homola, "Present and future of surface plasmon resonance biosensors," *Anal Bioanal Chem,* vol. 377, pp. 528-539, 5 June 2003.

[4] J. Homola, S. S. Yee, and G. Gauglitz, "Surface plasmon resonance sensors: review," *Sensors and Actuators B,* vol. 54, pp. 3-15, 1999.

[5] R. Donipudi, S. Pochiraju, and J. T. Hastings, "Self-Referenced SPR Sensing via Simultaneous Excitation of Long- and Short-Range Surface Plasmons," *Proceedings of the 2006 Conference on Lasers and Electrooptics,* 2006.

[6] R. Slavik, J. Homola, and H. Vaisocherova, "Advanced biosensing using simultaneous excitation of short and long range surface plasmons," *Measurement Science & Technology,* vol. 17, pp. 932-938, 2006.

[7] P. Adam, J. Dostalek, O. Telezhinakova, and J. Homola, "SPR sensor based on a bi-diffractive grating," *Proc. SPIE,* vol. 6585, 2007.

[8] J. T. Hastings, J. Guo, P. D. Keathley, P. B. Kumaresh, Y. Wei, S. Law, and L. G. Bachas, "Optimal Self-Referenced Sensing using Long- and Short- Range Surface Plasmons," *Optics Express,* vol. 15, pp. 17661-17672, 2007.

[9] W. C. Karl and H. H. Pien, "High-Resolution Biosensor Spectral Peak Shift Estimation," *IEEE Trans. On Signal Processing,* vol. 53, pp. 4631-4639, 2005.

[10] J. T. Hastings, "Optimizing Surface-Plasmon Resonance Sensors for Limit of Detection based on a Cramer-Rao Bound," *IEEE Sensors,* vol. 8, pp. 170-175, February 2008.

[11] D. Kim, "Effect of resonant localized plasmon coupling on the sensitivity enhancement of nanowire-based surface plasmon resonance biosensors," *J. Opt. Soc. Am. A,* vol. 23, pp. 2307-2314, 16 March 2006.

[12] P. B. Catrysse, G. GVeronis, H. Shin, J.-T. Shen, and S. Fan, "Guided modes supported by plasmonic films with a periodic arrangement of subwavelength slits," *Applied Physics Letters,* vol. 88, 16 November 2005.

[13] "Gram Determinant," in *Online Encyclopaedia of Mathematics*. vol. 2009, M. Hazewinkel, Ed.: Springer, 2002.

[14] P. Sheng, R. S. Tepleman, and P. N. Sanda, "Exact eigenfunctions for square-wave gratings: Application to diffraction and surface-plasmon calculations," *Physical Review B,* vol. 26, pp. 2907-2916, 15 September 1982.

[15] P. B. Johnson and R. W. Christy, "Optical-Constants of Noble-Metals," *Phys Rev B,* vol. 6, pp. 4370-4379, 1972.

[16] "Data sheet for N-BK7," Schott North America Inc., 2001.

[17] J. H. Lowry, J. S. Mendlowitz, and N. S. Subramanian, "Optical Characteristics of Teflon AF(R) Fluoroplastic Materials," *Optical Engineering,* vol. 31, pp. 1982-1985, 1992.

Vita

Authors Name – Phillip D. Keathley

Birthplace – Pikeville, Ky

Birthdate – June 25, 1986

Education

Bachelor of Science in Electrical Engineering

University of Kentucky

May 2009

Professional Positions/Research Experience

Nanoscale Engineering Certificate Program (U of K) Summer Research Program
Summer 2006

Center for Nanoscale Science and Engineering (CeNSE) lab technician – summer 2006 to summer 2007

National Science Foundation Research Experience for Undergraduates
Summer 2007 and Summer 2008

Undergraduate Research Assistant (U of K)
Fall 2007 – Spring 2008

Graduate Research Assistant (U of K)
Fall 2008 – Summer 2009

Scholastic/Professional Honors

Recipient of a National Defense Science and Engineering Graduate Fellowship (2009)

Astronaut Scholar 2008-09

Robert L. Cosgriff Award, Electrical Engineering Department, University of Kentucky

Alumni Leadership Scholarship 2008-09, Univeristy of Kentucky College of Engineering

Selected for 2006-07 Eta Kappa Nu Electrical Engineering Outstanding Junior award, Universityof Kentucky

Certificate of achievement from Nanoscale Engineering Certificate Program upon completion of curriculum and research with specialization in nanotechnology

Presidential Scholarship to the University of Kentucky from 2004 – ’08

Thurston H. Shrunk ('05 - '06) and Carl and Jody Kelly ('06 - '07 ; ’07 - ’08 ; ’08 - ‘09) scholarships from the University of Kentucky College of Engineering

Publications

P. D. Keathley and J. T. Hastings. Optical properties of sputtered fluorinated ethylene propylene and its application to surface-plasmon resonance sensor fabrication. American Vacuum Society. J. Vac. Sci. Technol. B Volume 26, Issue 6, pp. 2473-2477 (2008)

V. Karre, **P. D. Keathley**, J. Guo, and J.T. Hastings. Direct Electron Beam Patterning of Teflon AF. Conditionally accepted for publication in *IEEE Transactions on Nanotechnology*.

J.T. Hastings, J. Guo, **P.D. Keathley**, P.B. Kumaresh, Y. Wei, S. Law, and L. G. Bachas. Optimal self-referenced sensing using long- and short- range surface plasmons. Optics Express. Vol. 15 No. 26 (2007)

J. Guo, **P. D. Keathley**, and J. T. Hastings. Dual-mode surface-plasmon-resonance sensors using angular interrogation. Opt. Lett. **33**. 512-514 (2008)

Conferences/Presentations

P.D. Keathley and J.T. Hastings. Optical Properties Of Sputtered Fluorinated Ethylene Propylene. Electron Ion and Photon Beam Conference on Nanotechnology. Poster presentation. (2008)

Lineberry, Gene T., Lynch, A.L., **Keathley, D**., Wong J., Bettez, D. Fine-Tuning an Engineering Study Abroad Program. 37th ASEE/IEEE Frontiers in Education Conference. Session T1A. October 2007.